Abd el-aziz Khairy Abd el-aal, Farah Al-Jeri, and Abdullah Al-Enezi

Abstract

This chapter deals with all the precious documented recently published and unpublished studies that address the seismic situation and earthquakes in the State of Kuwait. Kuwait is geographically and geologically situated in the northeastern part of the Arabian Peninsula. In addition to being close to the famous Zagros belt of earthquakes, the local seismic sources inside Kuwait make it always vulnerable to earthquakes. We will review the instrumental and historical seismic records and the Kuwait National Seismic Network, including Data acquisition, data analysis, and data analysis. This chapter will also highlight all the recent seismic studies conducted in the Kuwait region. The induced seismicity, the seismic sources affecting Kuwait, as well as determining the types of faults using focal mechanism technique, specifying the seismic crustal models and ground motion attenuation inside Kuwait are being reviewed.

7.1 Introduction

The earthquake is one of the main common phenomena of natural risk. They have got consequences on nature, human existence, infrastructure, and buildings, (Bolt, 1993; Burton et al., 1978; Chung & Bernreuter, 1980; Hall, 2011; Kanamori, 2003). It represents 51% of the total damage of all-natural disasters. An earthquake is an unexpected slipping or motion of a portion of the earth's crust or violent moving of massive rocks known as plates (Fig. 7.1) underneath the earth's surface as a result of an unexpected release of stresses. The movement of tectonic plates releases stress that builds up along geological faults, causing earthquakes (Bath, 1979; Davison, 2014; Gubbins, 1990). Geologically speaking, a fault is a deep fracture that indicates the boundary between two tectonic plates, or it may be within the same plate. The main earthquake belts are located on the great faults between tectonic plates on the surface of the globe (https://en.wikipedia.org/wiki/Earthquake) as shown in Fig. 7.2. Many earthquake belts run along with coastal areas. Seismically, the point on the Earth's surface is fundamentally called the epicenter where the intensity of the earthquake and the devastation are strongest and greatest. The quantity of energy released by an earthquake is calculated by the seismic magnitude scale known as the Richter magnitude scale (Gutenberg & Richter, 1942; Richter, 1935). A big earthquake happens every few months somewhere in the world, but micro/small tremors occur constantly.

The earthquake (tremor or a quake) creates seismic waves (body waves and surface waves) (Bormann, 2012). The seismic activity or seismic record of an area indicates the frequency, type and magnitude of earthquakes over a certain period of time. The seismometer is used as a tool for measuring seismic recordings (Bath, 1979; Bormann, 2012). Moment magnitude is the most common of the various seismic scales in which earthquakes greater than magnitude of approximately 5 are reported. (Bormann, 2012; Hanks & Kanamori, 1979; Kanamori, 1977). The smaller earthquakes with magnitudes less than 5 are monitored through the national seismic networks and their magnitudes are calculated ordinarily on the local scale, commonly named the Richter scale (Gutenberg & Richter, 1942; Richter, 1935). Smaller earthquakes up to magnitude 3 are mostly imperceptible while the big earthquakes up to 6 and over potentially cause severe damage in/around the epicenter and over great distances, depending on their focal depth. The largest earthquakes throughout the ages are those whose magnitude exceeds 9, despite the fact that there is no restriction to the

A. el-aziz K. Abd el-aal (✉) · F. Al-Jeri · A. Al-Enezi
Kuwait Institute for Scientific Research (KISR), Safat, Kuwait
e-mail: akabdelaal@kisr.edu.kw; dewaky@yahoo.com

A. el-aziz K. Abd el-aal
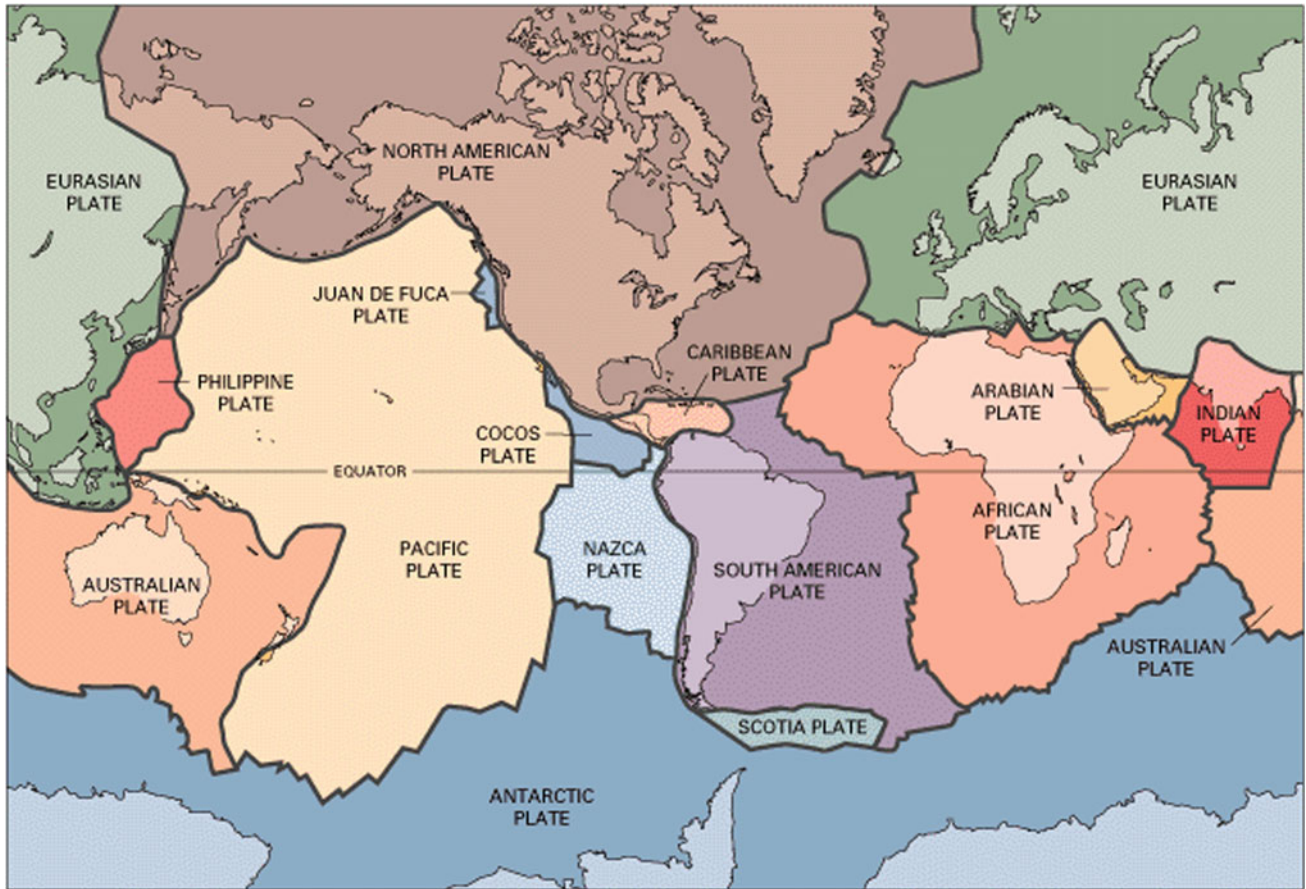National Research Institute of Astronomy and Geophysics, Helwan, Egypt

Fig. 7.1 The figure shows the boundaries of tectonic plates and also the continuous slow movement of these tectonic plates, the outer part of the Earth is what causes earthquakes and volcanoes
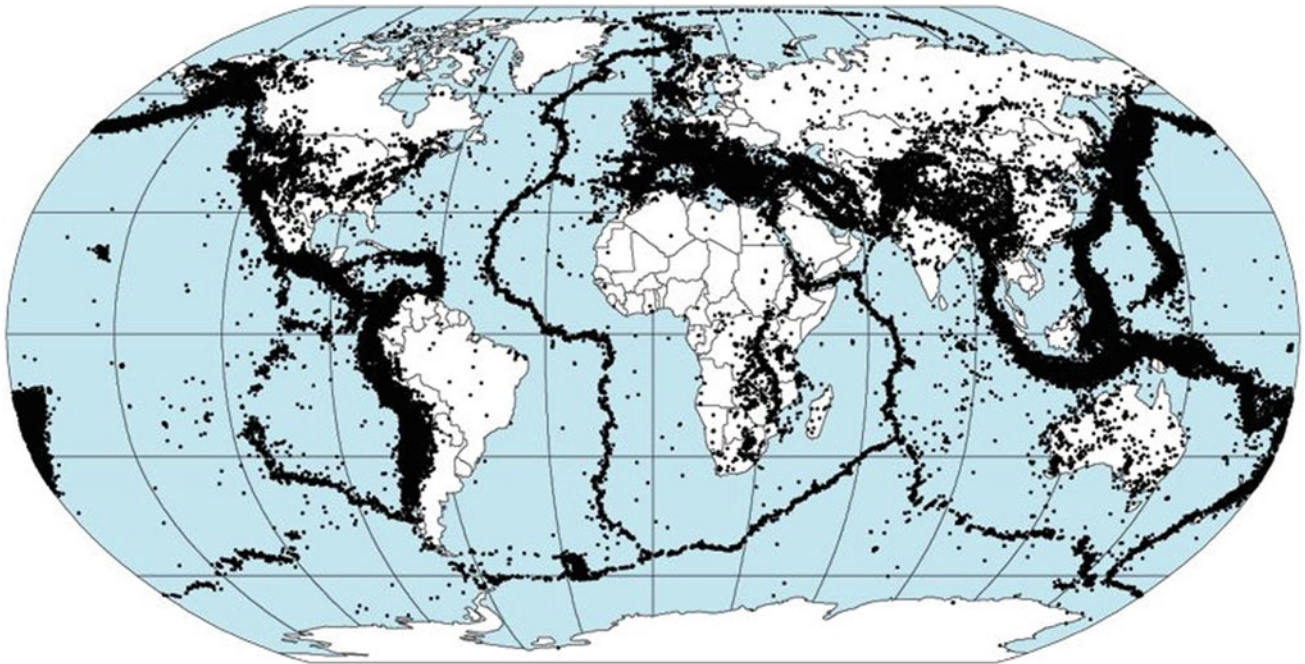

Fig. 7.2 Boundaries of plate tectonics, fire belts, and seismicity map of the earth

possible magnitude. When the hypocenter of a massive earthquake is positioned far from shore, the sea floor may shift sufficiently to cause a tsunami (Dudley & Lee, 1988; Levin & Nosov, 2009).

Earthquakes are classified as either tectonic or man-made (induced) events. Human and daily activities may cause induced earthquakes either directly or indirectly (Abd el-aal et al., 2020, 2021b). Earthquakes can also trigger landslides, and occasionally volcanic activity (Bath, 1979; Bormann, 2012). Earthquakes are generated by natural and man-made sources, including.

- Tectonic movement
  – Plate boundaries termed inter-plate earthquakes
  – Mid-continent, termed intraplate earthquakes
  – Mid-ocean ridge
- Volcanoes
- Reservoir induced
- Nuclear explosions

Scientists are researching ways to predict earthquakes, but their predictions are not always accurate (Allen, 1982; Kanamori, 2003; Lee et al., 2003). From this point, the earthquake occurrences still cannot be predicted reliably, but the characteristics of the earthquake's physical effects can be estimated (i.e., ground shaking, ground failure, surface fault rupture, landslides, regional tectonic deformation, tsunami waves, and aftershocks). Assessment of earthquake occurrence sequence hazard for any certain area plays an important role in proposing measures to minimize earthquake damage and to anticipate the future safe development of the strategic projects.

Particular attention should be paid to the assessment and the mitigation of the earthquake risk in seismically active areas, where monumental sites, human activities, and major investments are concentrated. The economic losses incurred by a devastating earthquake may cause a serious economic disruption with all its detrimental social consequences. Therefore regional as well as detailed urban planning in a seismic active area should rely on the proper knowledge of geological, geophysical, seismological, social and economical implications of the earthquake in the region.

An earthquake is a geodynamic phenomenon. The present seismic activity and the other geodynamic phenomena related to it (e.g., deformation and ruptures of the crust, volcanoes, geothermal manifestation, topographic features, etc.) are results of a relatively recent geologic process, which are usually, called active tectonic (Bath, 1979; Bormann, 2012). Very important information about tectonics can be obtained from the distribution of seismic activity. The main earthquake activity took place along the plate boundaries and recent active faults (Fig. 7.2).

7.2 Historical Earthquakes in Kuwait

Historically, and also by reviewing historical studies and manuscripts, where they never mentioned any strong earthquakes inside Kuwait, the international and regional seismic monitoring centers have recorded a number of small/medium earthquakes in Kuwait as shown in Table 7.1 and Fig. 7.3 (Abdelmeinum et al., 2004). In 1931, the first largest earthquake was recorded inside Kuwait by global monitoring stations and it was large and adequate enough to be monitored with a magnitude of 4.8 on the Richter scale located in the Boubyan island region. Although recent seismic studies after the establishment of the Kuwait network for seismic monitoring (KNSN) did not show seismic activity in the region in which the earthquake was recorded. This indicates that there may be an error in the coordinates and location of the earthquake. In 1973 an earthquake with magnitude 4.6 struck Kuwait and this event was located in the Arabian Gulf (Kuwait side). An earthquake with magnitude 4.1 took place in the same area (Abdelmeinum et al., 2004) in 1976. This was followed by two more earthquakes that were recorded by international agencies with magnitude 3.2 and 3.8 in the same year. The first event was located in northeast Kuwait and the second one was located in southeast Kuwait. After one year in 1977, there was an earthquake with magnitude 4.5 located in southeastern Kuwait (Table 7.1). In 1993 there was one of the most significant earthquakes that hit Kuwait is the Managish earthquake nearby Kuwait Saudi border in Southwestern Kuwait with magnitude 4.8 on the Richter scale (Abdelmeinum et al., 2004). It affected the surrounding areas, although the epicenter of the earthquake is about 150 km away from Kuwait City, but many of its residents have felt it, and some of the residents of the upper floors building have even been terrified, another earthquake in 1997 hit the same area, with a magnitude of 4.3 on the Richter scale and was felt by many citizens and residents. It was recorded by all the stations of the Kuwaiti National Seismic Network.

7.3 Instrumental Earthquake Recording in Kuwait

7.3.1 History of Seismic Recording

Instrumental recording of earthquakes started in Kuwait (1997). The Kuwaiti Government financed the Kuwait Institute for Scientific Research (KISR) to construct and deploy the Kuwait National Seismic Network (KNSN), which covers the whole Kuwaiti territory. KISR upgraded the data communication system from radio telemetry to

Table 7.1 Historical earthquakes recorded in Kuwait

Year	Month	Day	Time			Latitude	Longitude	Depth	Magnitude
			Hour	Minutes	Seconds				
1931	7	5	0	17	57	29.9	48.5	33	4.8
1973	3	14	1	16	44	28.5	49.1	5	4.6
1976	1	2	4	30	32	28.6	48.9	33	4.1
1976	9	26	0	12	47	29.9	47.3	33	3.2
1976	9	27	2	23	57	28.9	48.2	33	3.8
1977	1	16	20	31	26	28.8	48.1	5	4.5
1993	6	2	22	1	48	29	47.6	10	4.8
1997	9	18	20	24	51	28.9	47.5	10	3.9
1997	12	30	18	18	33	28.7	47.5	10	4.3

Fig. 7.3 Historical earthquakes recorded in Kuwait by international seismic center
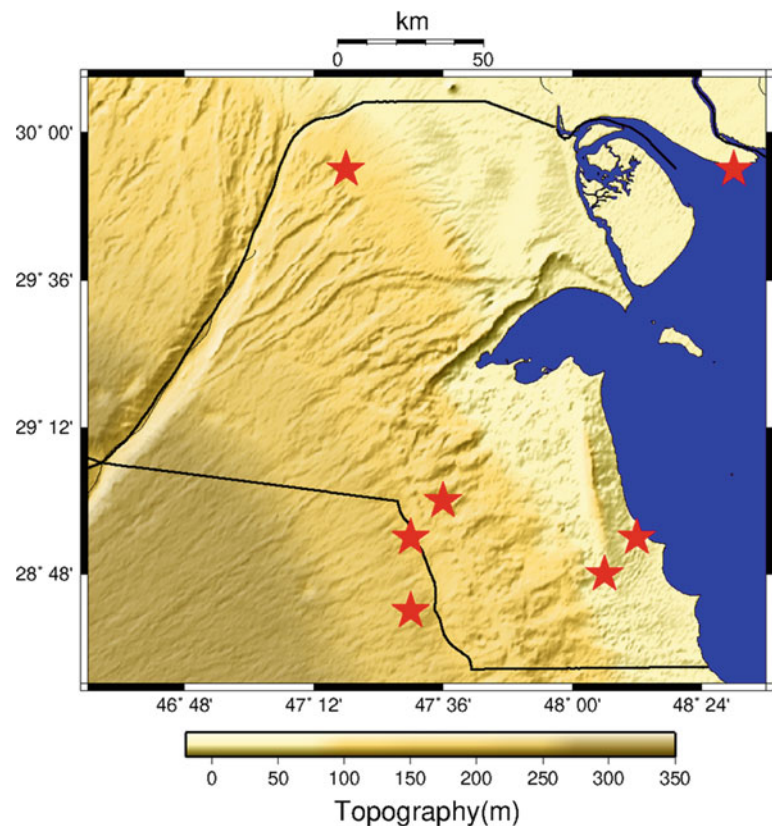
telephone leased lines to increase the efficiency of the KNSN.

In 1997, the KNSN was installed with seven short-period seismic stations and one broadband seismic station. Recently, the seismic stations of the KNSN were completely updated by replacing five short-period sensors with broadband sensors (KISR, 2019).

This network has enhanced the detectability level to record the microearthquakes and define their location precisely. Also, the KNSN contributes to define new seismic sources, which were not known before (KISR, 2019). From

the analysis of KNSN data, it was clear that the recording system was enhanced and developed in the last decade, and this development should be continued to achieve a complete record of earthquakes.

7.3.2 Kuwait National Seismic Network (KNSN)

7.3.2.1 KNSN Configuration

The KNSN network consists of the main center at KISR venue. With the beginning of the network's work, the

recorded seismic data was sent from field monitoring stations to the main center through wireless communications and recently, mobile phone lines were used in the data transmission process. The earthquake data received is processed and analyzed in order to derive the earthquake parameters, then saved and archived (Abd el-aal et al., 2020, 2021a, b; Al-Enzi et al., 2007; Gok et al., 2006; Gu et al., 2017, 2018; KISR, 2019).

Figure 7.4 illustrates the distribution of the field seismic monitoring stations which are installed in/around seismic sources as well as to cover Kuwait's country area as much as possible. Table 7.2 contains the sensor type, station code, coordinates and full name of the KNSN filed stations. At present, the KNSN network has equipped with two short-period sensors and six broadband sensors. The broadband sensors are from REFTEK 151-120A seismometer model and the short-period sensors are from SS-1 Range seismometer. Field seismic monitoring stations transfer continuous seismic dataset to the KNSN center at KISR venue over TCP/IP connection using a 5-G router. The main acquisition system at the KNSN receives seismic waveform data from both the Kinematrics and Reftek acquisition platforms (Abd el-aal et al. 2020, 2021a, b, c; Al-Enzi et al., 2007; KISR, 2019).

7.3.2.2 Data Acquisition

In the last five years, the Kuwait Earthquake Network (KNSN) has been fully and comprehensively developed and updated, where the SeisComP seismological software (https://www.seiscomp.de/) is used as a full-featured real-time seismic acquisition, processing, and analysis platform in the KNSN network (Fig. 7.5). The SeisComP system package has been established by Gempa (www.gempa.de) and GFZ German Research Centre for Geosciences (https://www.gfz-potsdam.de/en/) for earthquake data acquisition, distribution, processing and interactive analysis (KISR, 2019). The seismic data transmission protocol in SeisComP is the SeedLink. Among the SeisComP components are (1) automatic detection of earthquake events, (2) detection and determination of earthquake location and magnitude (3) automatic and manual processing facilities, which are enhanced by graphical user interface (GUIs) for visualization, seismic data quality control as well as rapid event review.

Features of SeisComP

The features of SeisComP (https://www.seiscomp.de/) include seismic data acquisition, waveform dataset recording and distribution, waveform real-time data exchange,

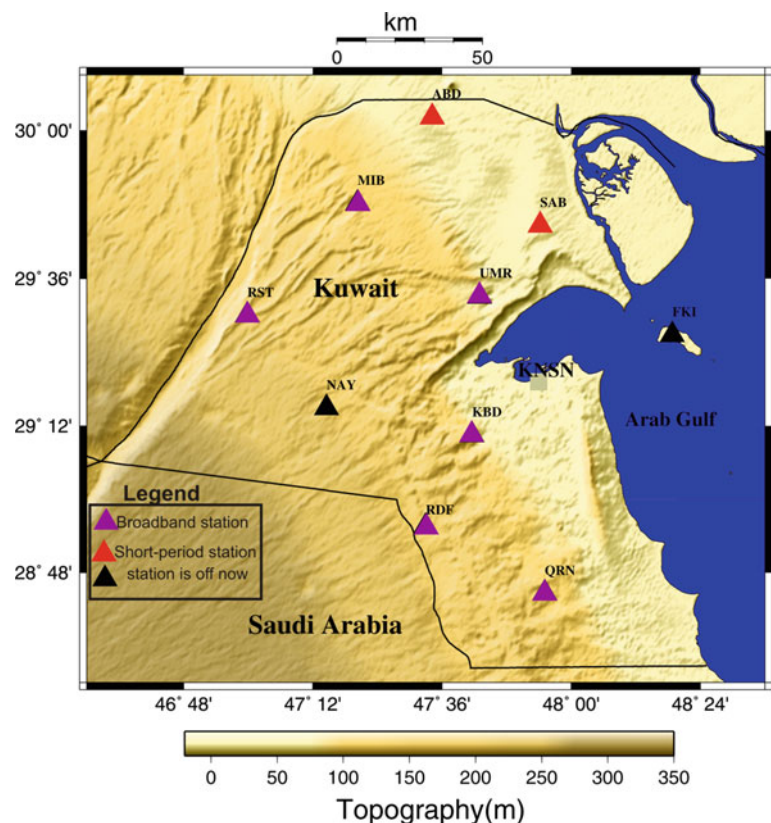**Fig. 7.4** Distribution of Kuwait National Seismic Network's stations

Table 7.2 Stations code and location of Kuwait National Seismic Network's Velocity-meter Units

Station	Code	Latitude	Longitude	Altitude (meter)	Sensor	Digitizer
KBD	9011	29 10.585	47 41.486	113	Reftek 151B	130S
QRN	9012	28 44.600	47 55.119	139	Reftek 151B	130S
RDF	9013	28 55.476	47 33.069	179	Reftek 151B	130S
RST	9015	29 30.024	46 59.87	216	Reftek 151B	130S
MIB	9016	29 48.135	47 20.402	120	Reftek 151B	130S
UMR	9017	29 33.201	47 42.972	85	Reftek 151B	130S
SAB	9018	29 44.616	47 54.240	53	Kinemetrics SS-1	130S
ABD	9019	30 02.193	47 34.178	62	Kinemetrics SS-1	130S
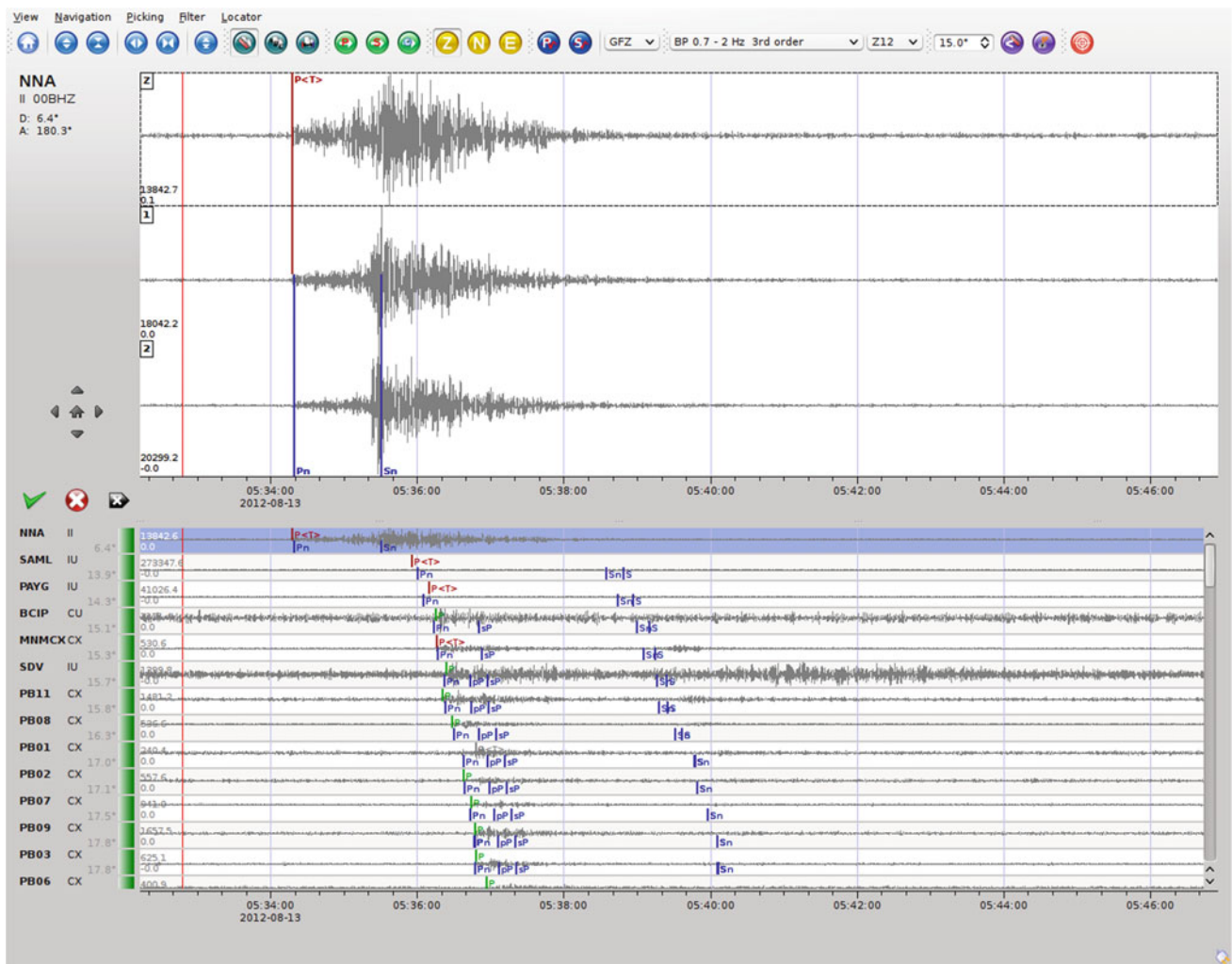
Fig. 7.5 Earthquake data processing using SeisComP software

monitoring and health network status, data processing, issuing of earthquake alerts and messages, complete seismic waveform archiving in miniSEED format, automatic and manual earthquake identification, event parameter archiving, and simple access to relevant details about waveforms, stations, and recent earthquakes (KISR, 2019). Throughout the seismic data analysis steps, the SeisComP initiates an input file that lists phases of each earthquake. The Hypoinverse program and other location software codes utilize in Seis-ComP with a set of files that give information related to the stations to be used in analysis, which is the crustal model that is suitable for earthquake location, as well as any delays, weights, or any corrections, should be to apply.

7.3.2.3 Data Processing and Analysis

The Kuwait Network KNSN recorded approximately more than 1027 local earthquakes since its inception in 2021, 548 of them before using the SeisComP platform in 2018. Before 2018, the SEISAN program (http://seisan.info/) was used to visualize and analyze earthquake data and save it after deriving seismic parameters, including the location and magnitude of the earthquake, and one of the appropriate programs from the HYPOINVERSE, HYPOCENTER (Lienert & Havskov, 1995) and HYPO71 (Lee, 1990) and was used for hypocenter detection (Al-Enzi et al., 2007). The P-wave and S-wave phase arrival times will be detected and selected using the waveform data from the KNSN in this analysis. Typically, using S-arrivals significantly improves earthquake solution accuracy especially location and focal depth. Because each of the sensors used has 3-components, the S-arrivals phases could be recognized without ambiguity. Consequently, the clear impulses of S-phases were mainly identified. Definitely, all earthquake events were essentially located using at least 5 P-wave picks and 2 S-wave picks. The large-time residuals resulting from phase readings of selected stations are always checked. Subsequently, the best events with (ERHs) and (ERZs) of less than 2 km have been selected for issuing the bulletin. Commonly, The RMS of the located earthquakes does not increase more than 0.3 s. The fundamental earthquake parameters (i.e., origin time, arrival time, travel time, location, depth and magnitude) of each earthquake were determined and archived.

7.3.2.4 Magnitude Scales in Kuwait

One of the most essential problems that seismologists face is detecting and selecting a perfect magnitude scale. Nowadays the SeisComP system used in KNSN has numerous adequate magnitude scales which can be used. Before SeisComP era, in the KNSN network, the duration (M_D) and local (M_L) magnitude scales are mainly chosen and used (Al-Enzi et al., 2007). In KNSN network, there was no standard magnitude scale therefore; duration magnitude scale was mainly used (Lee & Stewart, 1981):

$$M_D = 2\log D - 00.87 + 00.0035\Delta$$

where D refers to the total duration in seconds. The Δ expresses the epicentral distance in km. The duration of an earthquake is considered as the time from the first arrival onset to the time when the earthquake amplitude becomes the same as the pre-event amplitude. For each earthquake event, the announced magnitude is determined using all the magnitudes specified for each station. The local magnitude (M_L) relation that is used is the Hutton and Boore (1987) relation, which is close to the original Richter definition:

$$M_L = Log(amp) + 1.11 Log(D) + 0.00189D - 2.09.$$

where amp is the amplitude in nanometers and D is the hypocentral distance in kilometers. The scaling relationship between M_L magnitudes and with the body wave magnitude (M_b) of the National Earthquake Information Center (NEIC) of the United States Geological Survey (USGS) was fitted. M_L is related to M_b by the following relation (Al-Enzi et al., 2007):

$$M_b = 0.463 M_L + 2.449$$

7.4 Seismic Sources in and Around Kuwait

7.4.1 Local Seismic Sources

Modern and ancient seismic studies indicate that Kuwait is characterized by weak to moderate seismic activity in general. (Abd el-aal et al. 2020, 2021a, b, c; Al-enzi et al., 2007; Gu et al., 2017; Pasyanos et al., 2007). Before 1900, there are no documented manuscripts or seismic records for the State of Kuwait. During the twentieth century and before the establishment of the Kuwait Network for Seismic Monitoring (KNSN), some earthquakes were recorded inside Kuwait by the international seismological centers (Abdelmeinum et al., 2004). The dates and locations of these earthquakes are mentioned in detail in Sect. 7.2. The largest earthquake that was detected inside Kuwait was that in 1993 with a magnitude of 4.7 (Bou-Rabee & Nur, 2002). Some losses were reported in the infrastructure and public facilities, in addition to the extent of fear and panic that the citizens experienced as a result of their feeling of the earthquake (Abd el-aal et al. 2020; Gu et al., 2017; Bou-Rabee & Nur, 2002; Pasyanos et al., 2007). Figure 7.6 shows the seismicity of Kuwait.

Since the work of the network in 1997, there has been a very great possibility to monitor micro/small earthquakes with high accuracy inside Kuwait, which made it easy to identify and detect the local seismic sources inside Kuwait. The KNSN network has recorded more than 1,027

Fig. 7.6 Local seismic sources in Kuwait
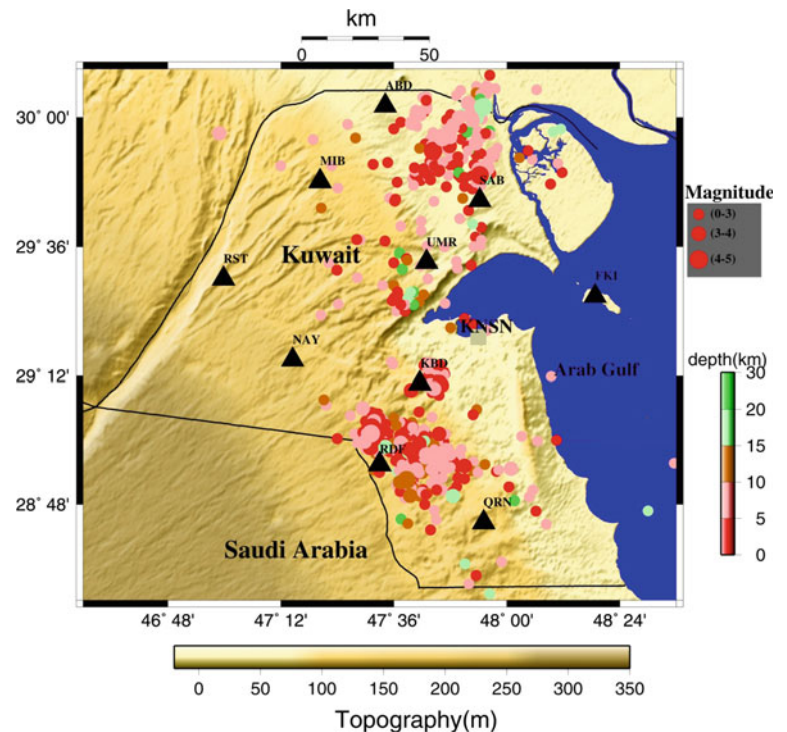
micro/small local earthquakes so far. By plotting the earthquake data on maps inside Kuwait, it was possible to identify two regions, one in the southwest of Kuwait named Minagish_Umm Gudair area and the other in the northeast of Kuwait, called Raudhatain-Sabriya area where earthquakes occur continuously (Fig. 7.6). Seismic studies conducted in Kuwait are still ongoing to find out the origin of these earthquakes and link their occurrence to the oil extraction process and from these studies (Abd el-aal et al. 2020, 2022; Al-enzi et al., 2007; Bou-Rabee, 2000; Bou-Rabee & Nur, 2002; Bou-Rabee et al., 2004; Gu et al., 2017; Pasyanos et al., 2007).

Although the phenomenon of earthquake swarming (sequence) is rare in Kuwait and did not occur only once, in the year 2019, where the KNSN recorded about 56 micro/small earthquakes that occurred on two consecutive days starting on the 15th of November (Fig. 7.7). The KNSN monitored 56 micro/small induced earthquakes sequence in the northern part of Kuwait having largest magnitude of 4.1 on the Richter scale, which hit Raudhatain-Sabriya area on 15 November 2019, at 23:47:26 Kuwait local time (Fig. 7.6). This earthquake occurred 7.4 km below the earth's surface. On the same day, the KNSN also recorded an earthquake of magnitude 4.0 on the Richter scale, which hit northern part of Kuwait. The earthquake hit at 14:47:37, Kuwait local time; it occurred 1.5 km below the surface of the earth. Many citizens and residents felt it in various parts of Kuwait. These earthquakes did not pose a threat.

The natural, artificial, and induced seismic activity recorded by KNSN from 1997 to 2019 in Kuwait (Fig. 7.6) reflects the incredible increase in the number of smaller earthquakes. This large number of events could be attributed to the 2019 earthquake sequence and road and infrastructure blasting which are defined as artificial earthquakes. Although the KNSN network has only a few seismic stations distributed in many remote sites, still the stations in operation give good azimuth coverage all over Kuwait's territory.

7.4.2   Regional Seismic Sources

Due to its geographical location in the northeastern part of the Arabian Peninsula, being the closest to the Zagros seismic belt, Kuwait is more affected by the earthquakes that occur in Iran and the Zagros belt (Fig. 7.8). Therefore, as a result of the collision between the Arab plate and the Eurasian plate, the rate of earth crust shortening is about 5 mm/year in the northwest of the belt, where it increases at a rate of 10 mm/year in southeast direction along the Zagros belt (Allen et al., 2004; Vernant et al., 2004). Small, medium, strong and destructive earthquakes occur along the Zagros belt and at different focal depths, including deep and shallow (Fig. 7.9). The Zagros belt extends from eastern Turkey to Oman in NW–SE direction with a length of 1500 km and a width of 200 to 300 km (Berberian, 1995; Hessami et al., 2003; Jackson & McKenzie, 1984).

Fig. 7.7 Location map of earthquakes sequence took place in 2019 in the northern part of Kuwait (after Abd el-aal et al., 2020)
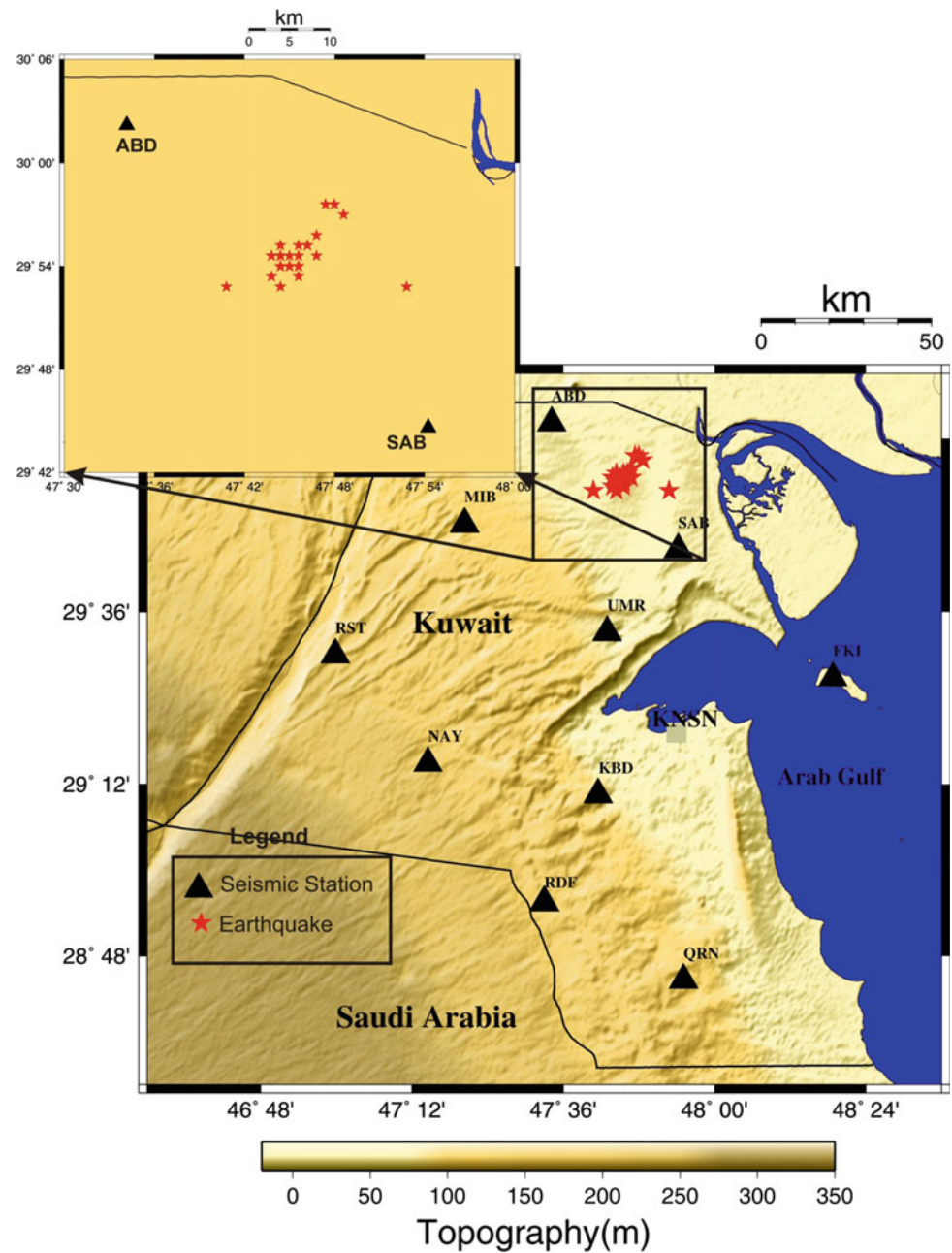
In general, the Zagros Thrust Belt (Zagros FTB) remains the largest seismic belt affecting Kuwait. As a result of the continuous movement on the Zagros FTB belt, earthquakes occur frequently, and their magnitudes range from moderate to strong and sometimes destructive.

The earthquakes recorded in the Zagros (FTB) region are characterized by being of shallow depths up to 20 km, especially in the north, and they increase in depth as we move towards the south (Engdahl et al., 2006; Hatzfeld et al., 2003; Kalaneh & Agh-Atabai, 2016; Talebian & Jackson, 2004; Tatar et al., 2004). Several scientists (e.g.

Berberian, 1995; Jackson, 1980; Jackson & McKenzie, 1984; Kadinsky-Cade & Barazangi, 1982; Ni & Barazangi, 1986) indicated that the mechanical fault plane solutions of the earthquakes that took place along Zagros FTB demonstrate that most seismic events occur on high-angle thrust faults (40°–50°) with strike parallel to the trend of the fold axes at the ground surface. Berberian (1995) pointed out that the major faults in Zagros FTB belt as shown in Fig. 7.10 are Main Zagros Reverse Fault (MZRF), Main Recent Fault (MRF) which are located in the northeastern boundary of the Zagros, High Zagros Fault (HZF), Mountain Front Fault
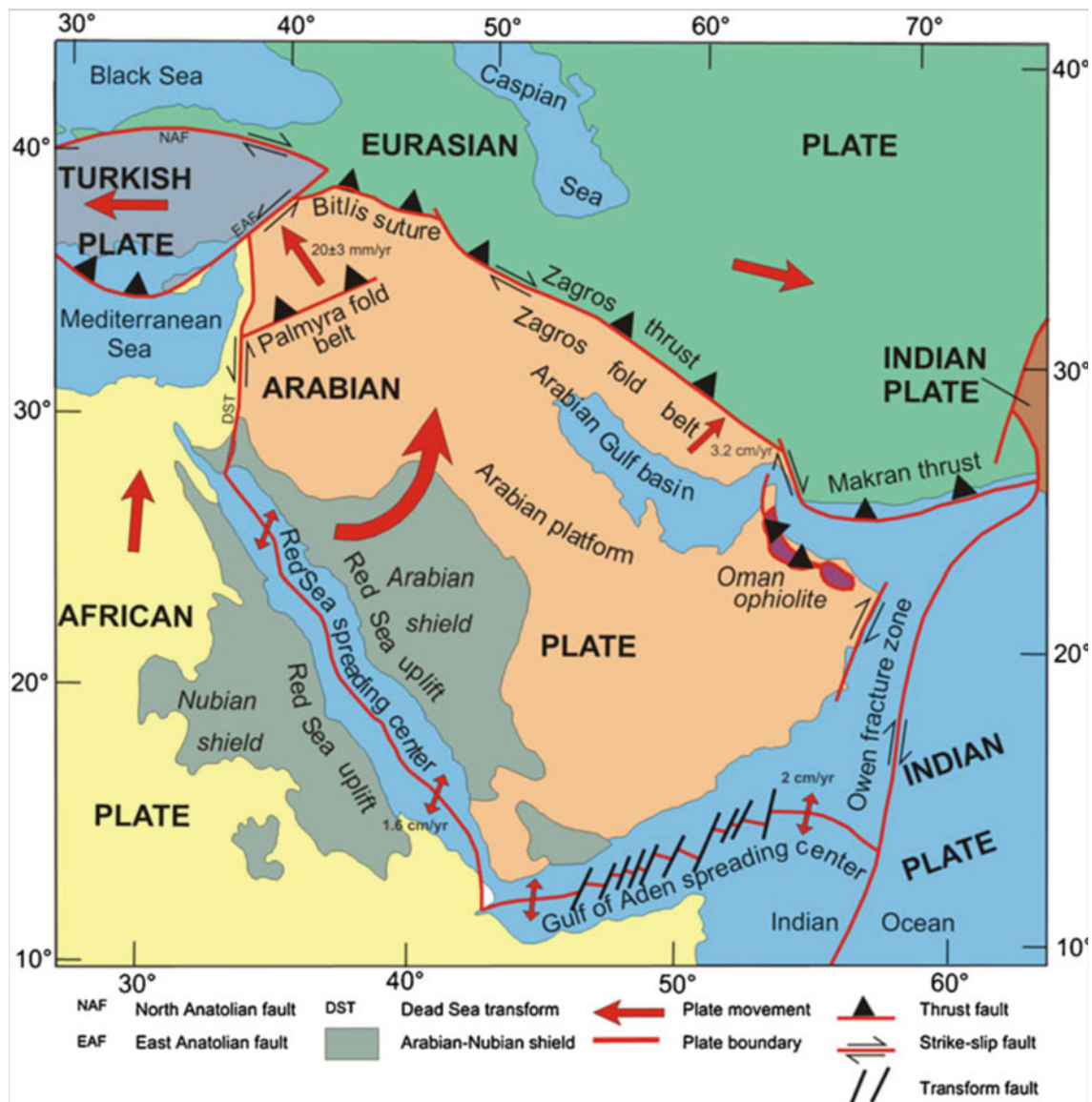
Fig. 7.8 The regional tectonic setting of Kuwait and its surrounding regions (after Johnson, 1998)

(MFF) and Zagros Foredeep Fault (ZFF). The Main Recent Fault (MRF) is a right-lateral strike-slip fault (Berberian, 1995).

Citizens inside Kuwait always feel regional earthquakes, especially the Zagros belt earthquakes, and despite the feeling of the earthquakes, they did not cause any damage, except for people's fear of them as they sometimes shake strongly the buildings (Abd el-aal et al. 2020, 2021c). Definitely, the famous Zagros belt FTB, which always causes moderate to strong earthquakes is far away and not at a small distance from Kuwait, however recently, as a result of the huge urban expansion inside Kuwait, especially the high-rise buildings and towers, people inside these buildings feel ground vibrations more than in the past. This may attribute to several factors, including that the high-rise buildings are

more sensitive to long-period seismic waves, and also the nature and characteristics of the soil and foundation layer beneath buildings play an important role, as it can lead to amplify the seismic waves if they are soft soil.

Earthquakes do not only occur in the Zagros belt zone, but also extend to the western coast of Iran on the Arabian Gulf, as the Kuwait seismic network and also global seismic networks always monitor earthquakes in this region along the coast, and these earthquakes are felt in Kuwait (Abd el-aal et al. 2020, 2021a, b; Engdahl et al., 2006). Earthquakes are also observed and recorded in the Arabian Gulf, but they remain few in number compared to the earthquakes recorded in the Zagros belt. On the other hand, in the western and southern sides of the State of Kuwait, where the Kingdom of Saudi Arabia, earthquakes are rarely detected in
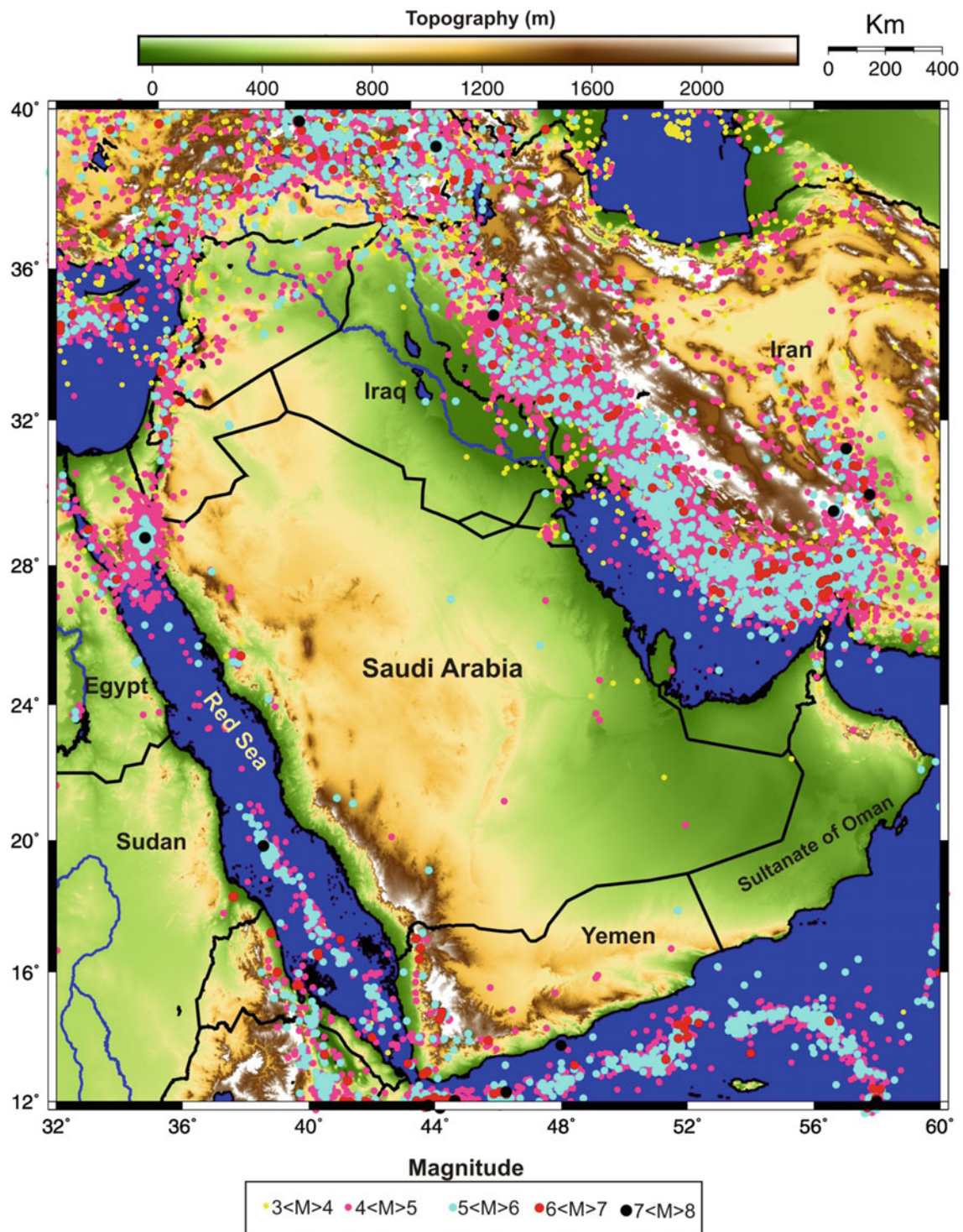
Fig. 7.9 Regional seismic activity with magnitude more than 4 in the Arabian Peninsula and adjacent areas to Kuwait was recorded from 1900 to 2020 (after Abd el-aal et al., 2021b)

this region and they do not pose any seismic hazard to the State of Kuwait.

As for the northern side, where the state of Iraq and the Iranian-Iraqi borders, earthquakes occur, and these earthquakes are felt in the State of Kuwait, especially if the earthquakes are moderate to strong even with magnitude greater than 5 if they are not close to the borders of Kuwait. Particularly, the Iraqi-Iranian border is considered the
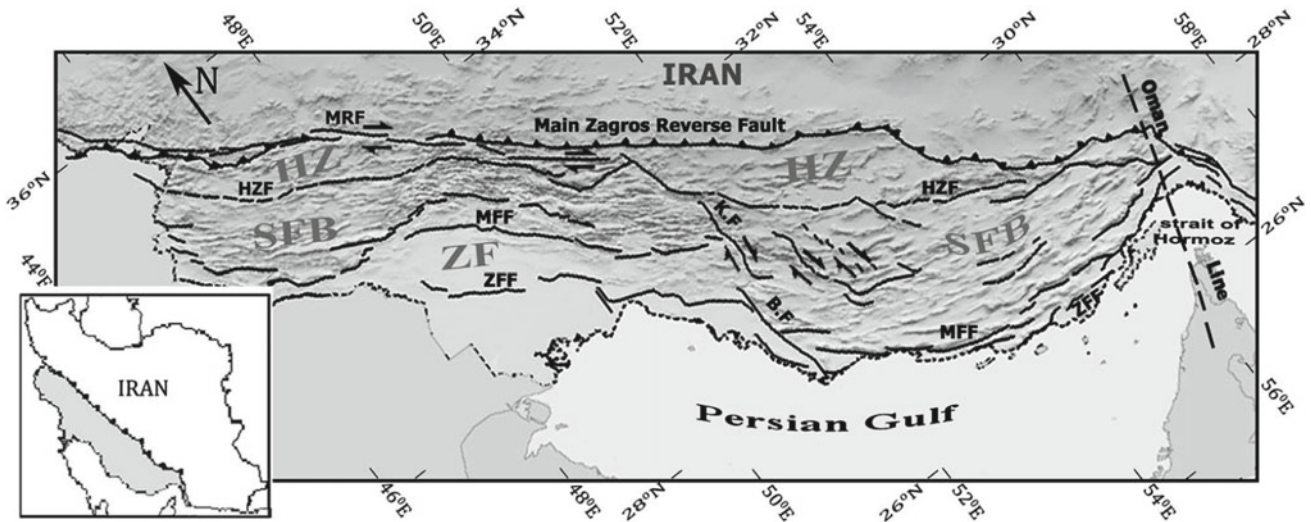
Fig. 7.10 Structure map of the Zagros thrust belt complied from the works of Kalaneh and Agh-Atabai (2016), Talebian and Jackson (2004), Berberian (1995)
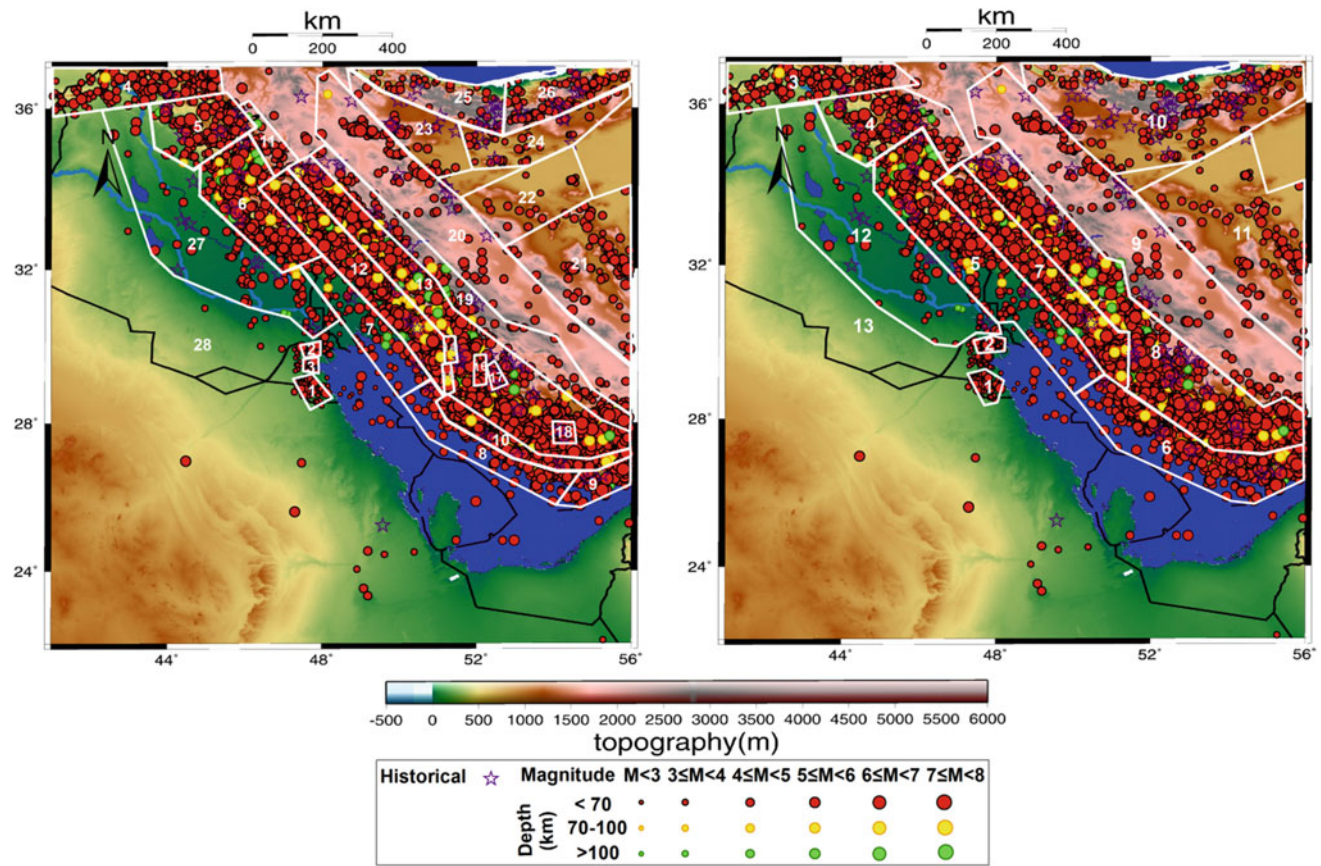
Fig. 7.11 Regional and local seismic sources in and surrounding Kuwait. The left panel represents the first proposed seismotectonic model while the right panel illustrates the second seismotectonic model (after Abd el-aal et al., 2022)

northern extension of the Zagros seismic belt, and therefore many strong earthquakes occur on it (Abd el-aal et al. 2020, 2021a, b, c; Engdahl et al., 2006; Gok et al., 2006; Gu et al., 2017, 2018; Kalaneh & Agh-Atabai, 2016; KISR, 2019).

Abd el-aal et al. (2022) conducted a study to detect and determine the effective local and regional seismic sources in and around Kuwait in two different scenarios of seismotectonic models (Fig. 7.11).

7.4.3 Regional Seismotectonic Setting

One of the most important seismotectonic elements surrounding the State of Kuwait is the Zagros (FTB) Belt, which is the most important tectonic region that greatly affects the State of Kuwait from the eastern side (Abd el-aal et al. 2020, 2021c; Engdahl et al., 2006; Gok et al., 2006; Gu et al., 2017, 2018; Kalaneh & Agh-Atabai, 2016; KISR, 2019). The Zagros FTB is a long zone of about 1,800 km and wide 300 km of the destroyed crusty rocks (Fig. 7.12) that were created at the front of the collision between the Eurasian tectonic plate and the Arabian tectonic plate within the Cretaceous/early Miocene epic (Garzica et al., 2019; Hessami, 2002; Hessami et al., 2003, 2006; Kalaneh & Agh-Atabai, 2016; Vergés et al., 2011). The Zagros FTB zone accommodates one of the largest oil regions in the world which comprise about 49% of the crude oil reserves found in thrust belts (FTBs) (Cooper, 2007).

7.4.4 Crustal Velocity Models in Kuwait

The earthquake velocity model and seismic structure of Kuwait region were studied by the scientists Al-Enzi et al. (2007), Pasyanos et al. (2007). They calculated the seismic velocity and seismic structures using the body-wave (P-and S-waves) waveform dataset of local and teleseismic events. The surface wave dispersion, receiver function and joint inversion were fundamentally used in this study. Indeed, the accuracy of earthquake locations, focal depths, and final network output "the bulletin" relies mainly on the accuracy of crustal models applied to find out the hypocenter
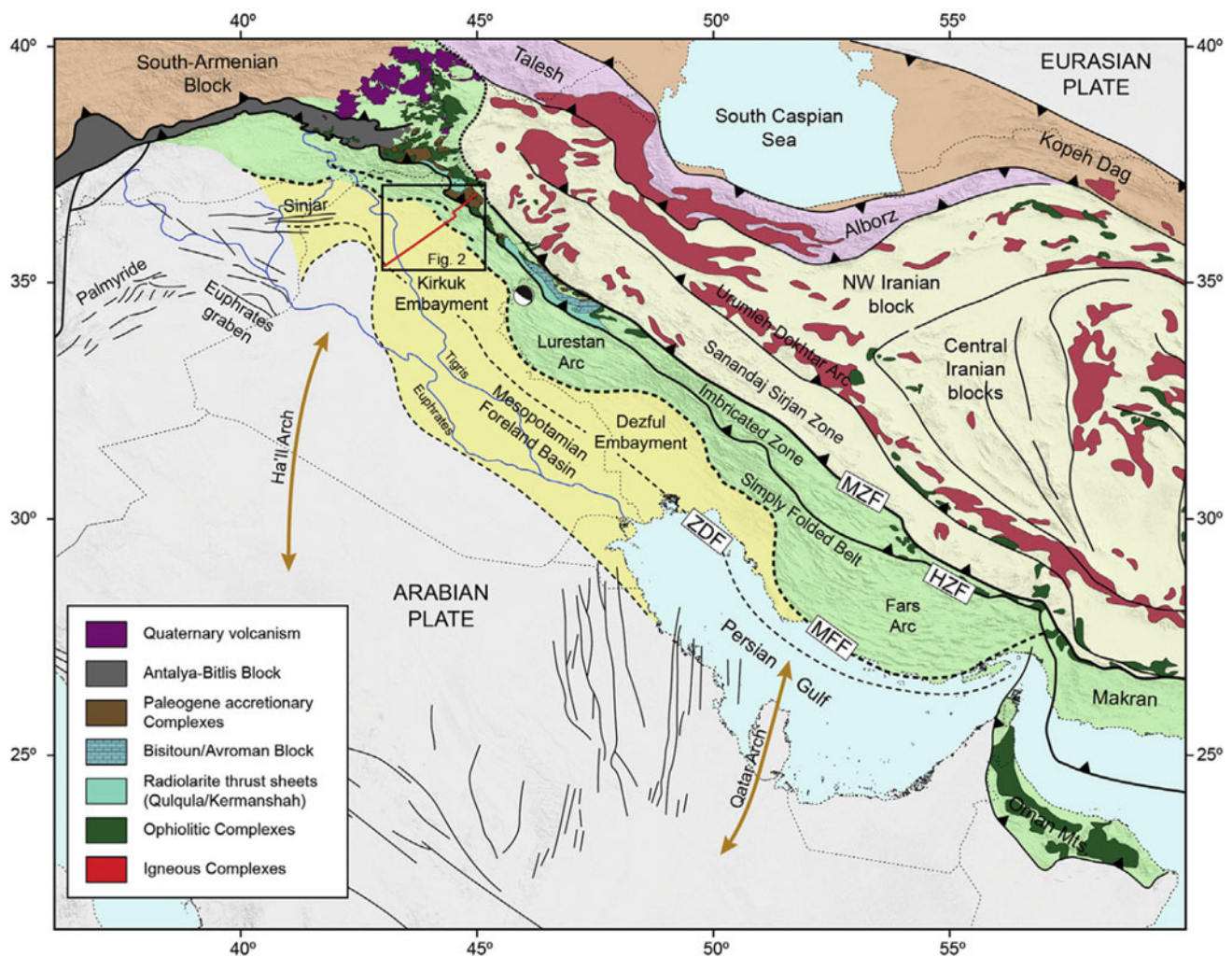

Fig. 7.12 The main tectonic units of Iran deformed between Arabia and Eurasia (after Garzica et al., 2019 which modified from Vergés et al., 2011)

parameters. The variation and difference in the geological structures and its components in the earth's crust and mantle lead to a difference in the velocity values of seismic waves. Al-Enzi et al. (2007) used the surface wave dispersion technique to group surface wave velocity for determining crust and upper mantle structures and seismic velocities in Kuwait region.

The seismic dataset recorded by the KBD broadband seismic station belongs to KNSN network principally used to create surface wave dispersion curves (Al-Enzi et al., 2007; Pasyanos et al., 2007). The use of the recorded seismic data from this station is only due to the absence of any other broadband stations in Kuwait. The authors applied surface wave dispersion using a robust technique called the multiple-filter analysis to calculate Surface Wave Group Velocities (SWGV) (Herrmann, 1973). A huge number of paths from Eurasia, Africa and Middle East were used in the calculations as shown in Fig. 7.13c. Dispersions on paths from the teleseismic and regional earthquakes inside the Kuwait area were measured. However, at the regional distance, most of the measurements were from regional earthquakes recorded from the Zagros seismic belt in Iran (plotted in the red colour paths in Fig. 7.13c). Pasyanos et al. (2001) tomographically used the conjugant gradient technique to invert all of the paths for lateral variation in the group velocity. Inversions were displayed as dispersion maps created separately for both the Rayleigh and Love waves having periods ranging from 7 to 100 s. An illustration map for the group velocity at 15 s Rayleigh waves is plotted in Fig. 7.13d.

It was found that at the KBD station site, there are very slow Love and Rayleigh waves group velocities at short periods, indicating, the presence of dense sediments in this region (Pasyanos et al., 2007) (Fig. 7.14). The authors pointed out there are great matches and comparisons between the 15 s Rayleigh wave group velocity map illustrated in Fig. 7.14d and the sediment thickness illustrated in Fig. 7.13b. Dispersion data were used to invert parameters of the crust and upper mantle in Kuwait. Pasyanos et al., 2007 stated that the obtained results from inversion of surface wave mainly fit with an earth model has a 44 km crustal thickness (Fig. 7.15): It is distributed as 4-km-thick sediments over 40-km-thick crustal layers with a seismic velocity gradient of 0.75 km/s (i.e., 3.0 km/s velocity contrast over 40 km). The upper mantle in the region has a P-wave velocity of 7.8 km/s (i.e., 4.3 km/s S-wave velocity).

The second scheme used by Al-Enzi et al. (2007), Pasyanos et al. (2007) is the Receiver function method (RF). Certainly, the Receiver functions have become famous and very effective in determining the velocity and thickness of the lithosphere and the earth's crust under any seismic recording station (Ammon et al., 1990; Langston, 1979;

Owens et al., 1984). Fundamentally, the technique of Teleseismic Receiver Function (TRF) separates converted P-to-S-waves from the incident P-wave. Thus it is determined by deconvolving the vertical component from the radial component. This approach is sensitive and robust for determining local structures within 100 km of the monitoring station.

Al-Enzi et al. (2007), Pasyanos et al. (2007) calculated the receiver function at station KBD for teleseismic events. The use of epicentral distances for all the earthquakes used in the study ranged between 60 to 85°, gave a steep angle of incidence for the P-waves.

The authors engaged three main groups of earthquake events from in/near the Japanese islands, southwestern Pacific, and from south region of southern Africa (Fig. 7.16).

Al-Enzi et al. (2007) concluded that the results obtained from the inversion of receiver function varied extensively among the stacks from different back azimuths. The study showed that there is a very large difference between inferred velocities in the upper and lower parts of the earth's crust as well as the upper part of the mantle. For this reason the authors (Al-Enzi et al., 2007; Pasyanos et al., 2007) combined two schemes datasets into one inversion approach implementing the joint inversion results (Fig. 7.17).

The KUW1 velocity model was mainly constructed by Al-Enzi et al. (2007) for the Kuwait region. The KUW1 Model is illustrated in green colour in Fig. 7.18 with details in Table 7.3.

Al-Enzi et al. (2007), Pasyanos et al. (2007) concluded that a thick sedimentary column was found, which were classified into two layers. A 17-km-thick upper crust with P-wave seismic velocity equal to 5.89 km/s and S-wave seismic velocity equal to 3.40 km/s exists in the crystalline crust, while the middle crust has a 9-km-thick with P-wave seismic velocity equal to 6.41 and S-wave seismic velocity equal to 3.70, and the lower crust with P-wave velocity = 6.95 km/s and S-wave velocity = 3.90 km/s has 11-km-thick. The total crustal thickness was 45 km. The study shows that beneath the Moho zone, the P-and S-seismic velocities in the upper mantle have 7.84 km/s and 4.4 km/s (Al-Enzi et al., 2007). The results were mainly compared to other seismic velocity profiles for Kuwait region (Fig. 7.18).

The first two models basically investigate the sedimentary thickness. However, three layers in the region have thicknesses of 0.93, 4.00, and 2.35 km, while the P-wave velocities of 2.53, 4.02, and 5 km/s have been characterized in the Laske sediment model (Laske et al., 2001) (magenta lines). Other seismic models take into account the profile of the entire Earth's crust. The CRUST2.0 seismic model shown in black is the first model (Laske et al., 2001). The CRUST2.0 model basically distinguishes this area as
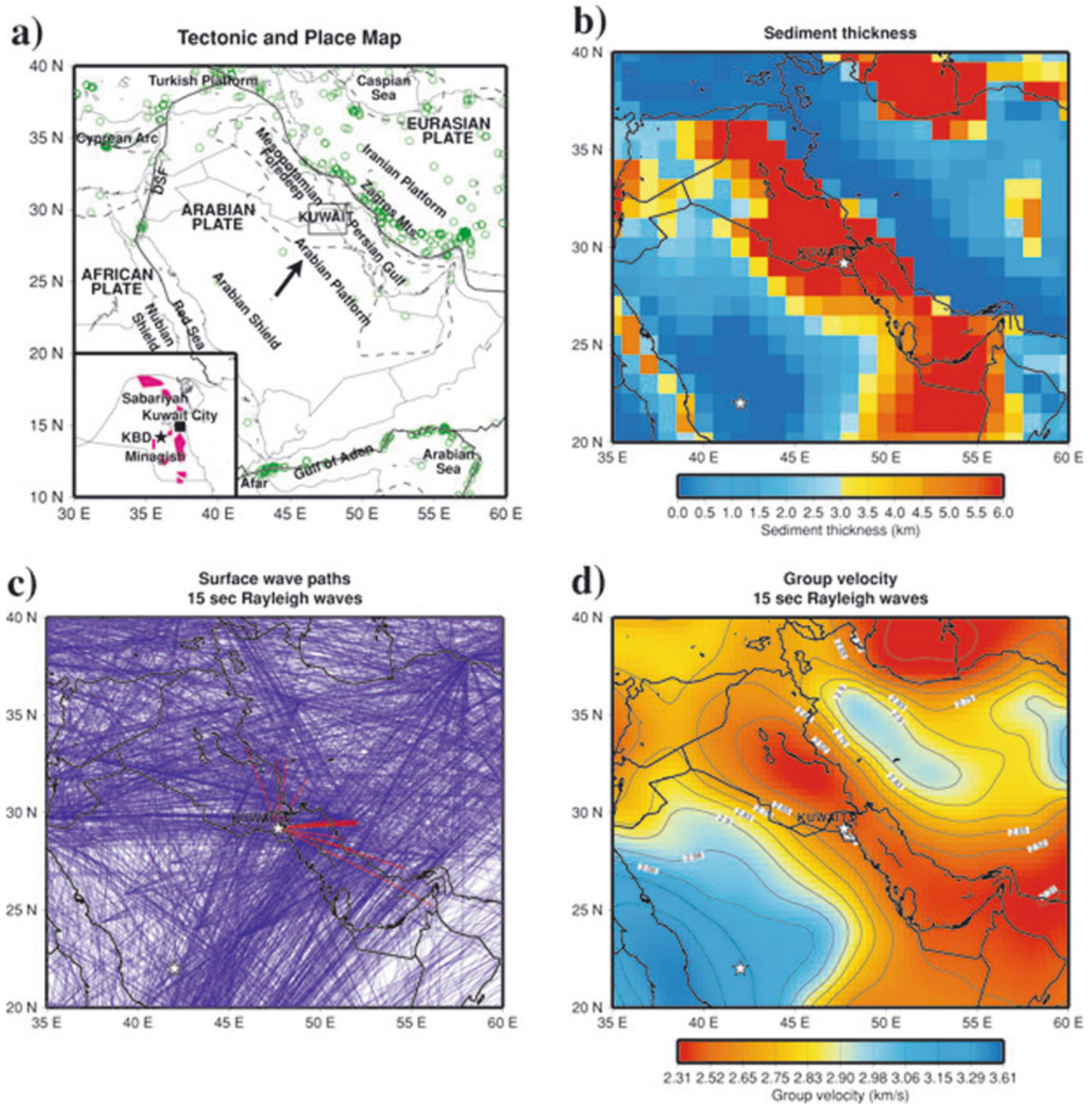
Fig. 7.13 Panel **a** tectonic and structure map of the Arab Peninsula and its surroundings. The star symbol in the map refers to KBD station while the circle symbols represent recent seismicity (events $M \geq 5.0$ from 1990 to present). The dashed lines designated areas have sediment thicknesses of more than 5 km, while the solid lines refer to tectonic plate borders. Panel **b** shoes the thickness map of sediment of the Arab Peninsula and its surroundings from Laske et al. (2001). Panel **c** shows path map of the Rayleigh wave group velocity dispersion measurements at 15 s. The red lines indicate regional paths monitored at station KBD. The Star symbol refers to the place of the profiles illustrated in Fig. 7.14. Panel **d** illustrated the Rayleigh waves group velocities at 15 s obtained from tomographic inversion (after Pasyanos et al., 2007)
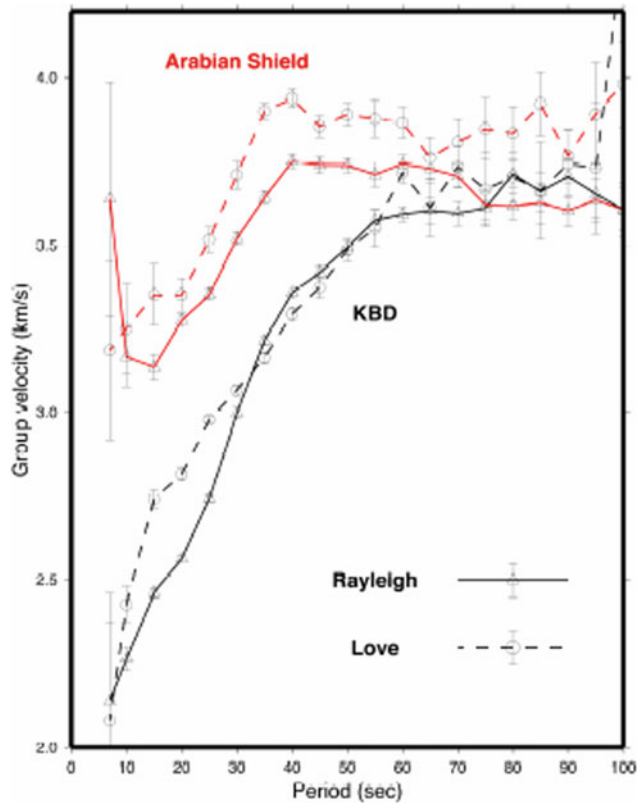
Fig. 7.14 Rayleigh wave group velocities at station KBD (black lines) while the red lines at the Arabian Shield location (after Al-Enzi et al., 2007)

DA, In other words, it is a primary model that has 6 km-thick layers. The crust in the area in this specific model is about 41 km-thick with seismic velocities of 5.88 km/s and 3.28 km/s for P- and S-wave, respectively. Thereupon, the seismic velocities of the mantle below the Moho are of 8.2 km/s and 4.7 km/s.

The crustal model in red colour which is picked from Bou-Rabee (2000) is mainly obtained from CRUST5.1 (Mooney et al., 1998). The sediment thickness in this model is about 7 km, while the thickness of the crust is approximately 40 km; however, the average body-wave seismic velocities of the upper mantle have 8.0 km/s and 4.49 km/s respectively. The crustal model of the Arabian Platform (AP) is an average model for the Arabian Platform and is completely considered from the regional waveform modeling paths from the Zagros seismic belt which was recorded in central Arabia (Rodgers et al., 1999). This model is illustrated on the figure in cyan colour. The model of Pasyanos et al. (2004) is shown in blue is mainly considered from the WENA model.

### 7.4.5 Focal Mechanism Solutions and Stress Pattern

To understand the nature of seismic sources in Kuwait, focal-mechanism solutions, of the local earthquakes that occurred in Kuwait, are significantly needed. The faults that cause earthquakes are mainly under the Earth's surface, however, they may extend to the ground surface. Outgoing seismic waves are affected by the stress distribution in/near the source, thus imparting asymmetry to distant sites. This of course will lead to the assumption of radiation patterns (Lay & Wallace, 1995). The radiation pattern can be typically defined as a geometric description of the wave amplitude and sensation of the initial motion distribution on the P-and S-wave-fronts near the source (Fig. 7.19). However, the shear dislocation with low order symmetry presents inferring a predictable relationship between radiation pattern of seismic wave motion and orientation of fault-plane, allowing the identification of faulting processes remotely.

The focal-mechanism of earthquake provides details fundamental to understanding the nature and origin of the seismic event. The focal-mechanism solution of earthquake permits stress mode to change in the ground to be identified from far distances at the exact time and location of the earthquake. Accumulation of focal-mechanism solutions (i.e., details about fault slip and fault orientation) have revealed the kinematic behavior of seismic zones, and led to research on the seismological implications of global tectonics (Fig. 7.20).

Al-Enzi et al. (2007) conducted a study to prepare focal-mechanism maps for earthquakes in Kuwait, the available phase readings, or seismograms, of the KNSN were used. Thirty-three earthquakes were selected according to the accuracy of their location, clearness of first pick and number of minimum recording seismic stations (Al-Enzi et al., 2007). Those events were recorded in at least 6 stations. Generally, the accuracy of focal-mechanism determination increases as the number of stations increases. The selected events were grouped into two groups according to focal depth the first group included events that were located at depth of less than 6 km, and the second group included events that were located at depths of more than 6 km.

To construct the focal mechanism of an event's source, the PMAN program was used. In constructing the fault-plane solution for an earthquake, 3 parameters were used the type of polarities of the first onset P-wave from waveform data at numerous stations, source-to-station azimuths for those stations, and takeoff angles (AIN) for the P-wave rays traveling from the earthquake focus towards the station. AIN determination requires knowledge of the P-wave velocity with

Fig. 7.15 Velocity dispersion results of surface wave using inversion technique. The upper lift panel shows the receiver-function data fit while the dispersion data are shown in lower lift panel. The velocity model is illustrated at the right panel (after Al-Enzi et al., 2007)
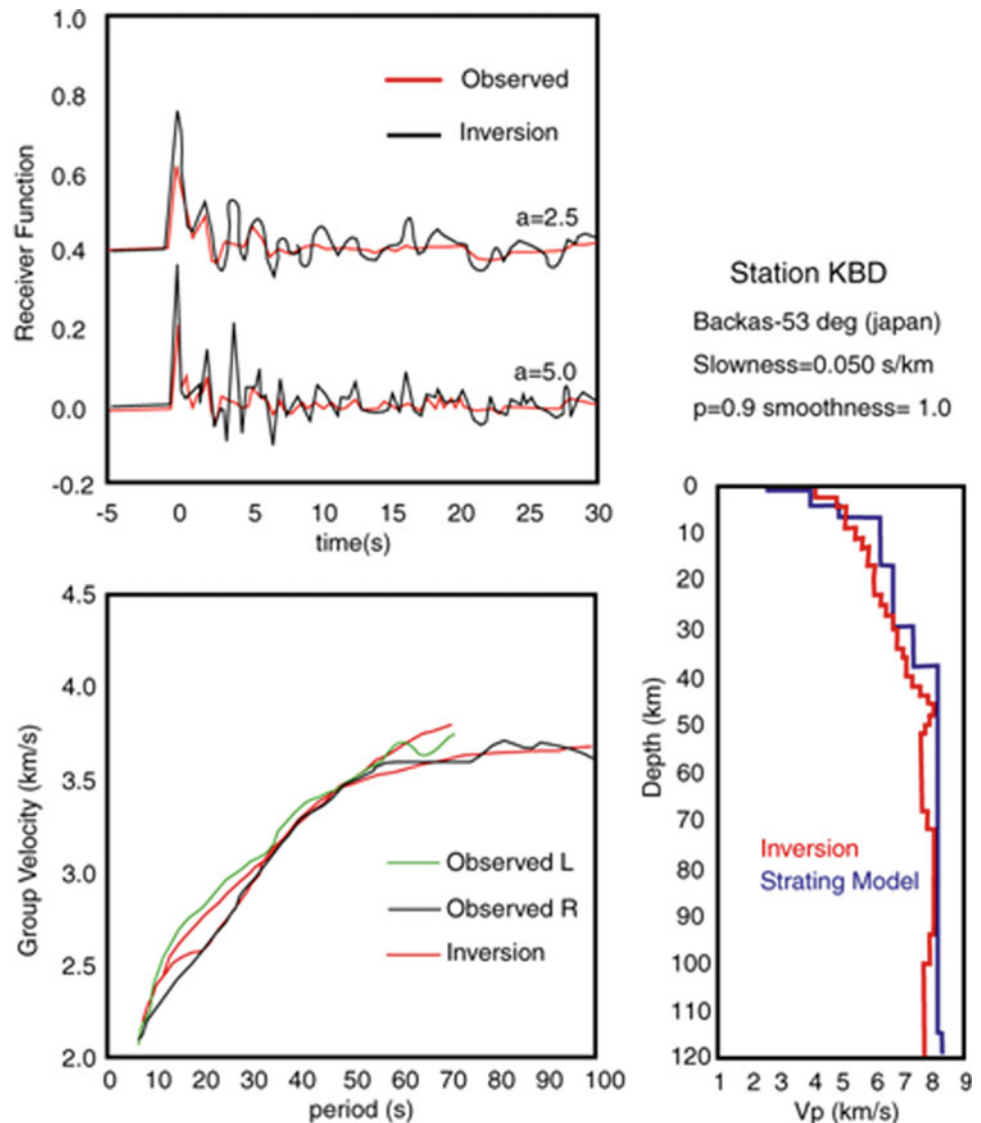
depth. The used seismic velocity model in the source area significantly affects AIN calculation for rays incoming at a certain seismic station. The use of inaccurate seismic velocities model may lead to errors in the separation of fault planes and also not setting the polarity readings of the stations in the correct quadrants. The AIN angles were calculated by using the newest crustal model developed for Kuwait.

Due to the lack of stations that cover the area and the low magnitudes of the recorded events, the fault-plane solutions of individual events were uncontrolled. So, composite fault-plane solutions were made to overcome the uncontrolled fault-plane solutions of individual events. Six composite diagrams were prepared in this study, 2 for the first group (S1 and S2) and 4 (D1 to D4) for the second group (Al-Enzi et al., 2007). Composites indicate to reverse and normal focal mechanisms. Such structures are not observed

in the exposed surface. At the southern region, the composites of events which have depths of more than 6 km (D1, D2 and D3) are distinguished by a normal faulting with a strike-slip element (Fig. 7.21). In turn, the composite (S1) of seismic events located at depths of less than 6 km is distinguished by a reverse faulting with minor component of strike-slip. The two composites (S2 and D4) for the northeastern region are characterized by reverse mechanisms, although the events were located at different depth levels. These mechanisms reflect the domination of compression forces in the northern part of Kuwait, consistent with the general trend of forces in the area toward the subduction zone along the Zagros Mountains (Al-Enzi et al., 2007).

Abd el-aal et al. (2021a) prepared a study regarding the phenomenon of earthquakes sequence that occurred in the northern part of the State of Kuwait, and this phenomenon is rare and occurred for the first time in Kuwait since the
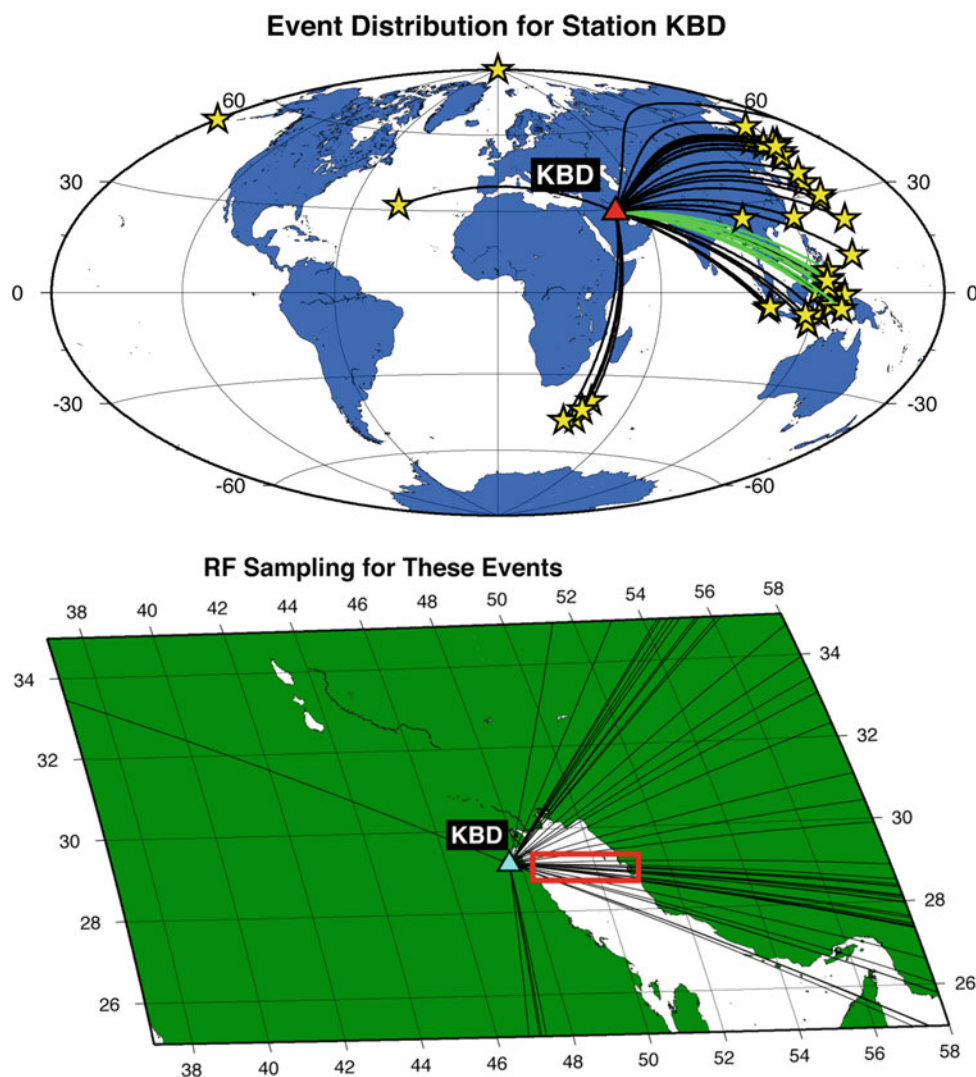
establishment of the KNSN network. On November 15, 2019, for two consecutive days, the KNSN recorded a number of micro/small earthquakes, numbering more than 56. Only 29 earthquakes were selected from the sequence in terms of the number of recorded stations, their magnitudes, and the accuracy of the location of the selected earthquakes. The study was carried out by Abd el-aal et al. (2021a), including the determination of earthquake properties in terms of source parameters, fault type and fault orientation, as well as the determination of moment magnitudes using modern geophysical methods such as moment Tensor and inversion techniques, in addition to determining the pattern of the stresses in the region.

Abd el-aal et al. (2021a) identified the two largest earthquakes in the group, with moment magnitudes 4.4 and 4.5, respectively. The study indicated that one from the two earthquakes is deeper in focal depth than the other. Fourteen earthquakes were purified and selected for focal mechanism process based on the quality of the waveform and minimum required station number. The study indicated that the fault causing earthquakes is of the normal fault type with a minor strike-slip element. The study also showed that the fault takes NE-SW direction, and this direction fully corresponds to the distribution, clustering and shape of the earthquakes sequence illustrated in Fig. 7.22 (Abd el-aal et al. 2021a). The researchers stated that the obtained results indicated that this seismic sequence has a human component equivalent to the tectonic component as assigned from the CLVD and the ratio of DC components in addition to the obtained values of the stress drop (Abd el-aal et al. 2021a). All the results obtained from the study indicate that these earthquakes are of the type "triggered seismicity" and also fully agree with the geological and structural situation in the region (Abd el-aal et al. 2021a). The authors also pointed out Kuwait contains many oil production fields, but earthquakes do not occur except in certain places with pre-existing faults in the northern and southern regions and not from others (Abd el-aal et al. 2021a).
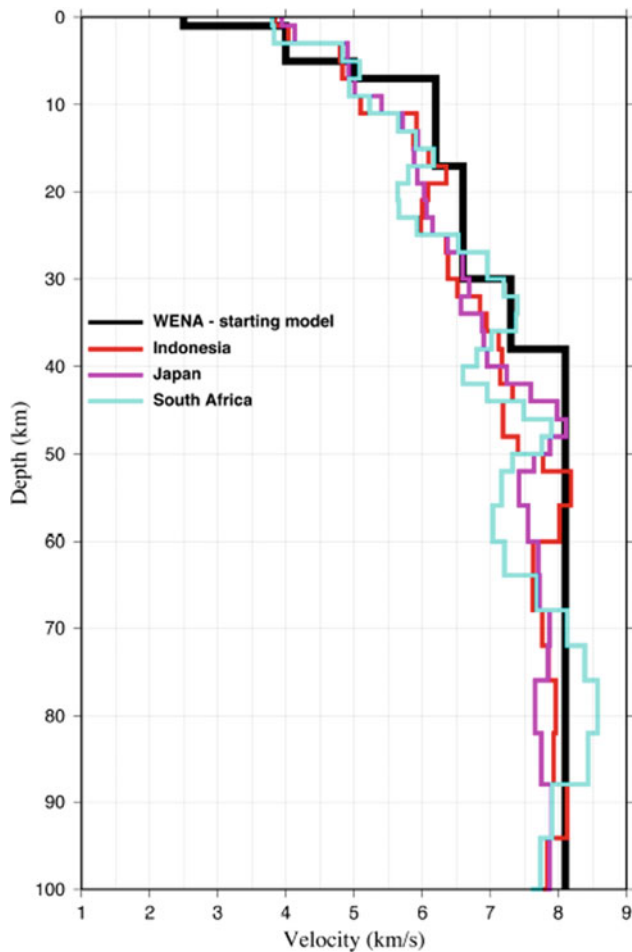
Fig. 7.17 Joint inversion scheme for receiver function and surface wave datasets (after Al-Enzi et al., 2007)

The geological structure and tectonic situation in the region, where the earthquakes sequence took place, may be approximated by considering the stress pattern throughout the release of energy from earthquake events (Abd el-aal et al. 2021a). The authors mainly estimated the stress style from the focal mechanism solutions of the earthquakes sequence presented in Fig. 7.22 by means of the software code-named STRESSINVERSE of Vavrycuk (2014). The software code utilizes Michael's method (Michael, 1984) which is robust and accurate to determine the stress axes direction. This powerful procedure can provide reasonable accuracy of the stress axes estimation, even if the focal mechanism solutions are randomly picked (Fojtikova & Vavrycuk, 2018; Fojtikova et al., 2010). The fault-plane solutions of nearly 14 earthquakes from the earthquake sequence are fundamentally applied to recognize the stress style in the area (Fig. 7.23).

The stress distribution in the region where the earthquake sequence occurred was mainly determined from the focal mechanism solutions of 14 earthquakes by performing the stress tensor procedure. The main stress axes directions are shown in Fig. 7.23, while Table 7.4 contains their obtained values. Therefore, the estimated results in Fig. 7.23 display that the axis σ_1 has a nearly vertical plunge taking direction SSE, while the axis σ_3 shows a vertical plunge in main direction SWW (Fig. 7.23). A schematic diagram of Mohr circle presented in Fig. 7.23 panel (b), demonstrated that the estimated fault planes are principally clustered on the failure criterion area called Mohr–Coulomb, proofing that the analyzed dataset are consistent with the fault instability model (Vavrycuk, 2011, 2014; Vavrycuk et al., 2013). The results obtained from stress tensor pointed to the predictable shape ratio is about 0.53 and the friction is about 0.4 on the faults for the earthquake sequence as revealed in Fig. 7.23 panel (d).

7.5 Conclusion

In this chapter, we review the most important works, outputs and results that specifically pertain to the Kuwait seismicity. There are really a few works on this subject. Kuwait is located on the Arabian Gulf in the northeast corner of the Arab peninsula. Actually, studying and monitoring seismic activity in Kuwait started recently in 1997. There is no record of historical earthquakes in Kuwait. Many scientists believe that the local seismic activity in Kuwait is closely related to the process of extracting oil from Kuwait. Especially the local earthquakes inside Kuwait are characterized by small/minor magnitudes and shallow focal depths.

Seismic studies in Kuwait indicate that there are two regions where local earthquakes occur. The Minagish_Umm Gudair region is located in the southwest of Kuwait, and the Raudhatain-Sabriya region is located in the northeast of Kuwait. Kuwait is constantly exposed to regional earthquakes from the famous Zagros belt.

In this chapter, we summarized most of the works that dealt with the seismological situation in Kuwait, as well as the history of seismic monitoring in Kuwait.

Fig. 7.18 The figure shows comparison between the seismic velocity model named KUW1 and different seismic velocity models from regional regions. The seismic velocity model (KUW1) is plotted in green colour. The regional seismic models include the CRUST2.0, A P, WENA, sediment, and Kuwait model which are plotted in black, cyan, blue, magenta, and red respectively. The black arrows in the right panel demonstrate the sedimentary layers from Bou-Rabee (2000), Al-Enzi et al. (2007)
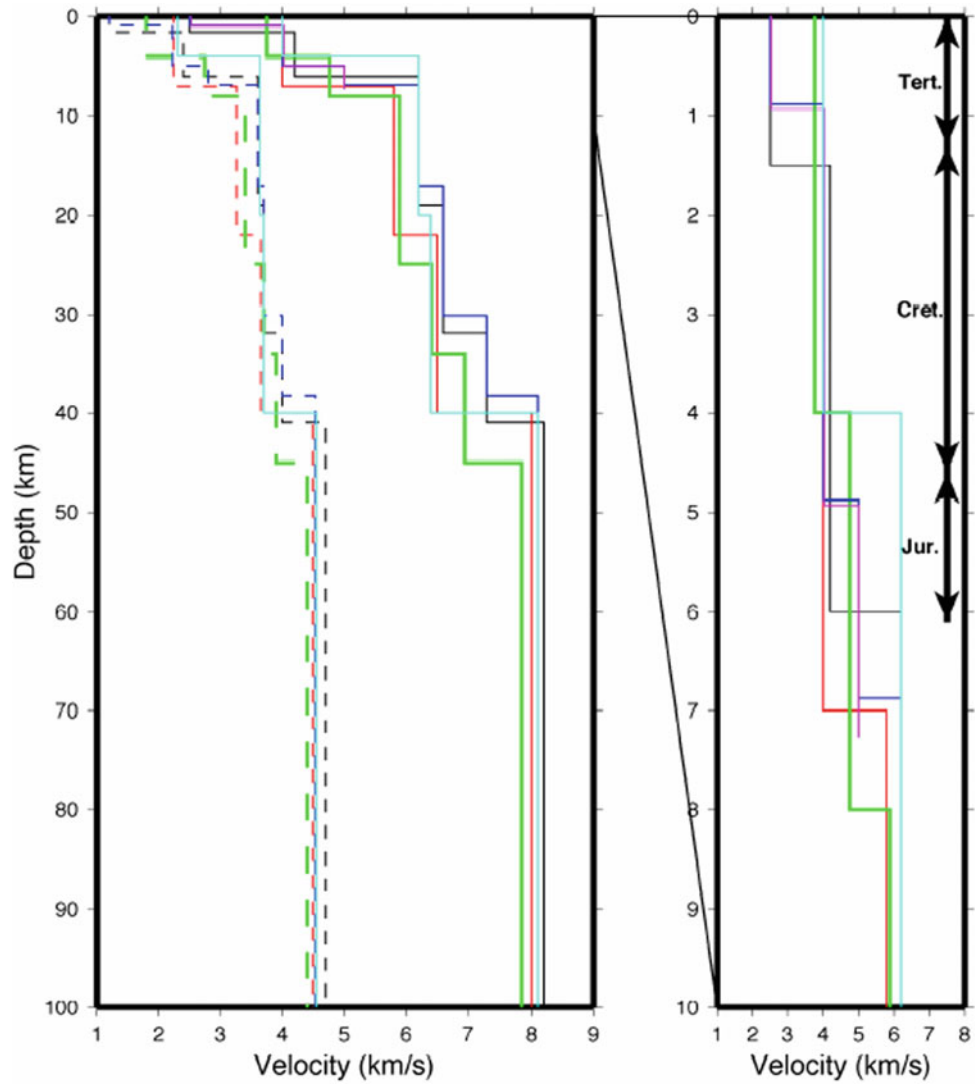

Table 7.3 Outline of the seismic models for Kuwait region and its vicinity. Label refers to colour or symbol used in Fig. 7.18 (after Al-Enzi et al., 2007)

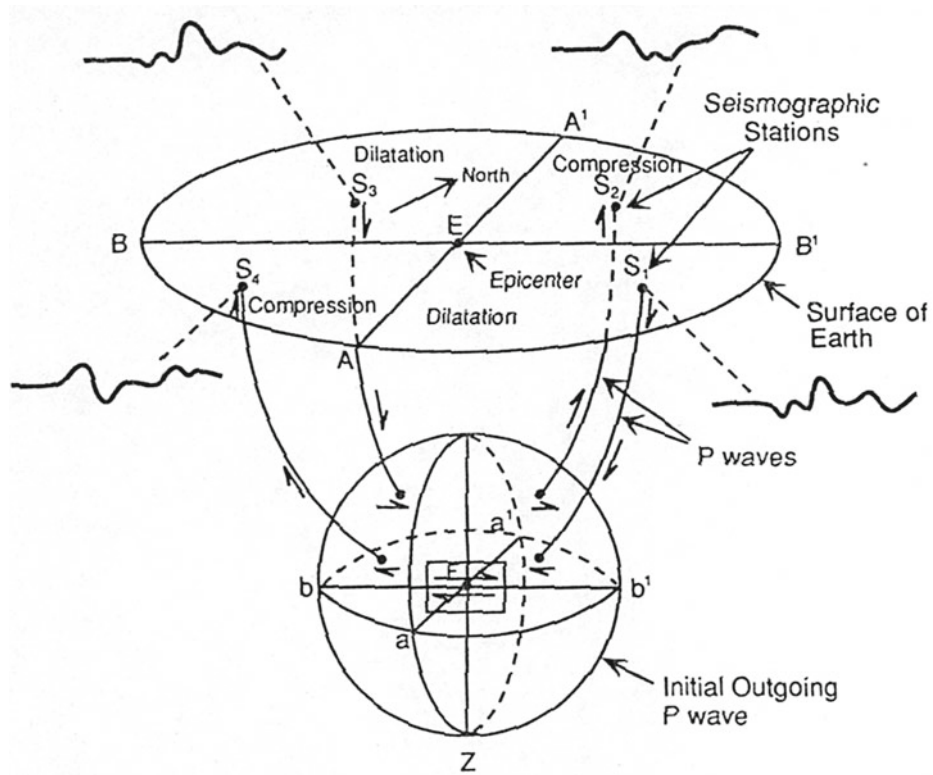| Model	Label	Sediment Thickness (km)	Average Crustal Velocity (km/s) (P-/ S-wave)	Crustal Thickness (km)	Upper Mantle Velocity (km/s) (P-/ S-wave)
Laske sed	Magenta	7.3	*	*	*
Sed. Profile	Arrow	6.1	*	*	*
CRUST 2.0	Black	6	5.88/3.28	41	8.20/4.7
Kuwait	Red	7	6.18/3.47	40	8/4.49
WENA	Blue	7	6.18/3.31	38	8.1/4.58
AP	Cyan	4	6.07/3.5	40	8.1/4.55
KUW1	Green	8	5.96/3.38	45	7.84/4.44

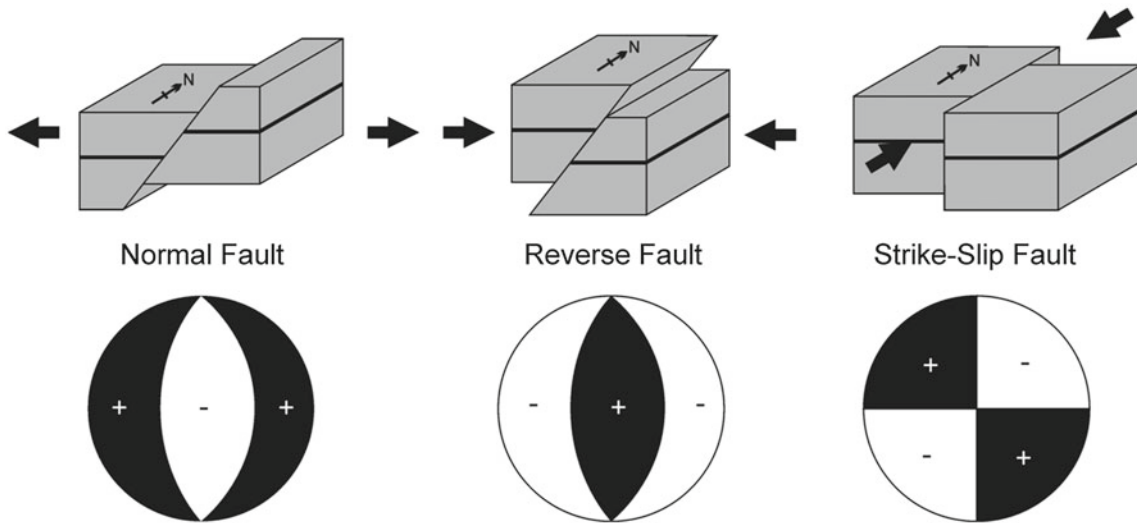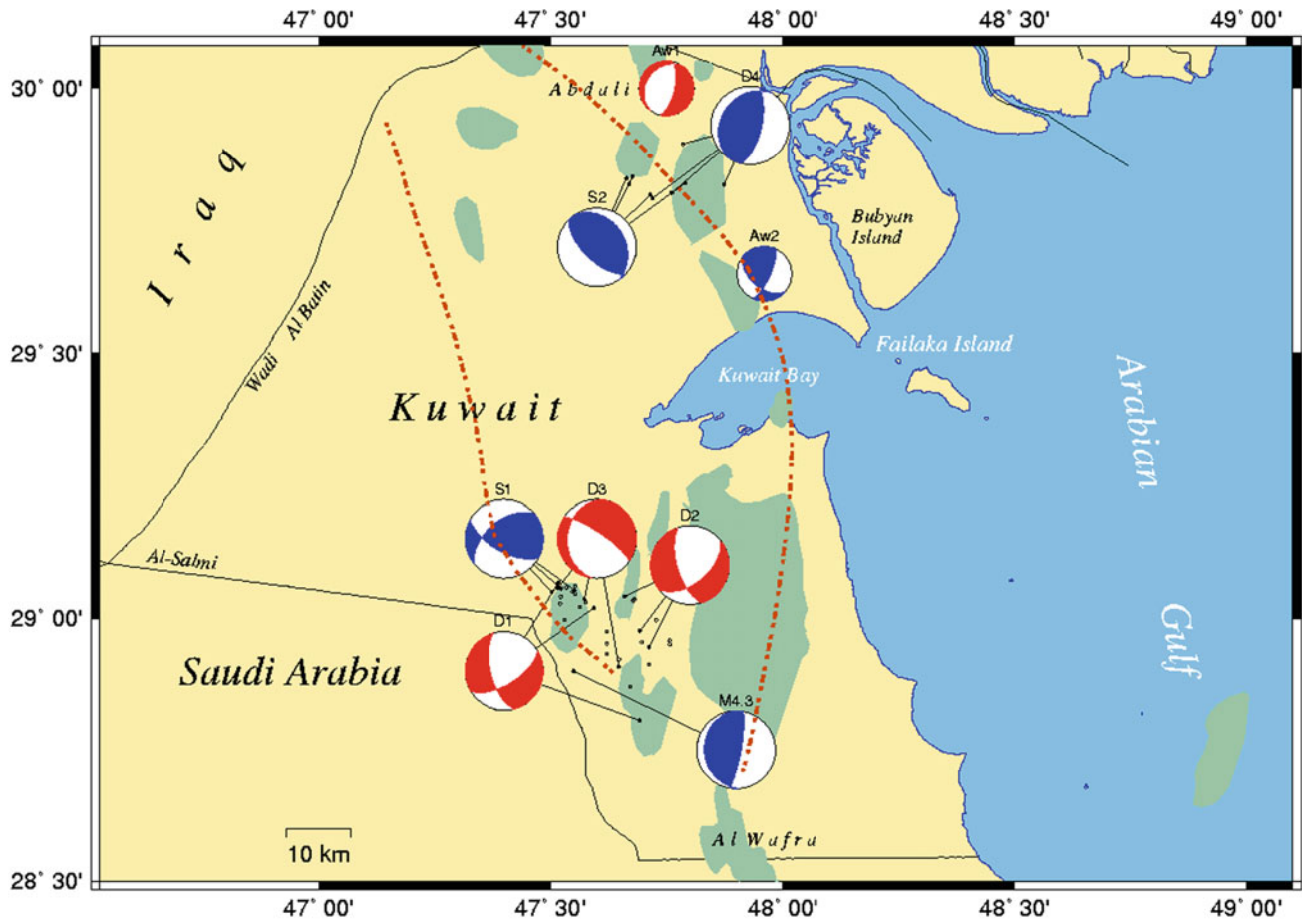**Fig. 7.19** Three-dimensional variation of P-and S-wave amplitude and polarity on a spreading wavefront source

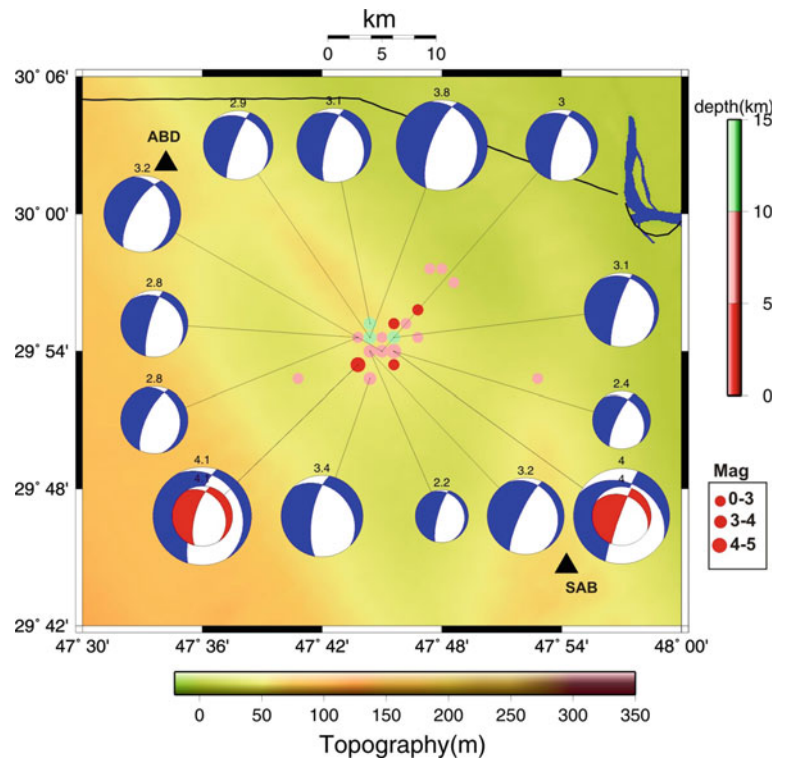**Fig. 7.20** Diagram illustrates the type of faults and their focal mechanism solutions

Fig. 7.21 Focal mechanism solutions of the earthquakes in Kuwait (after Al-Enzi et al., 2007)

Fig. 7.22 Focal mechanism
solutions of the earthquake
sequence took place at the
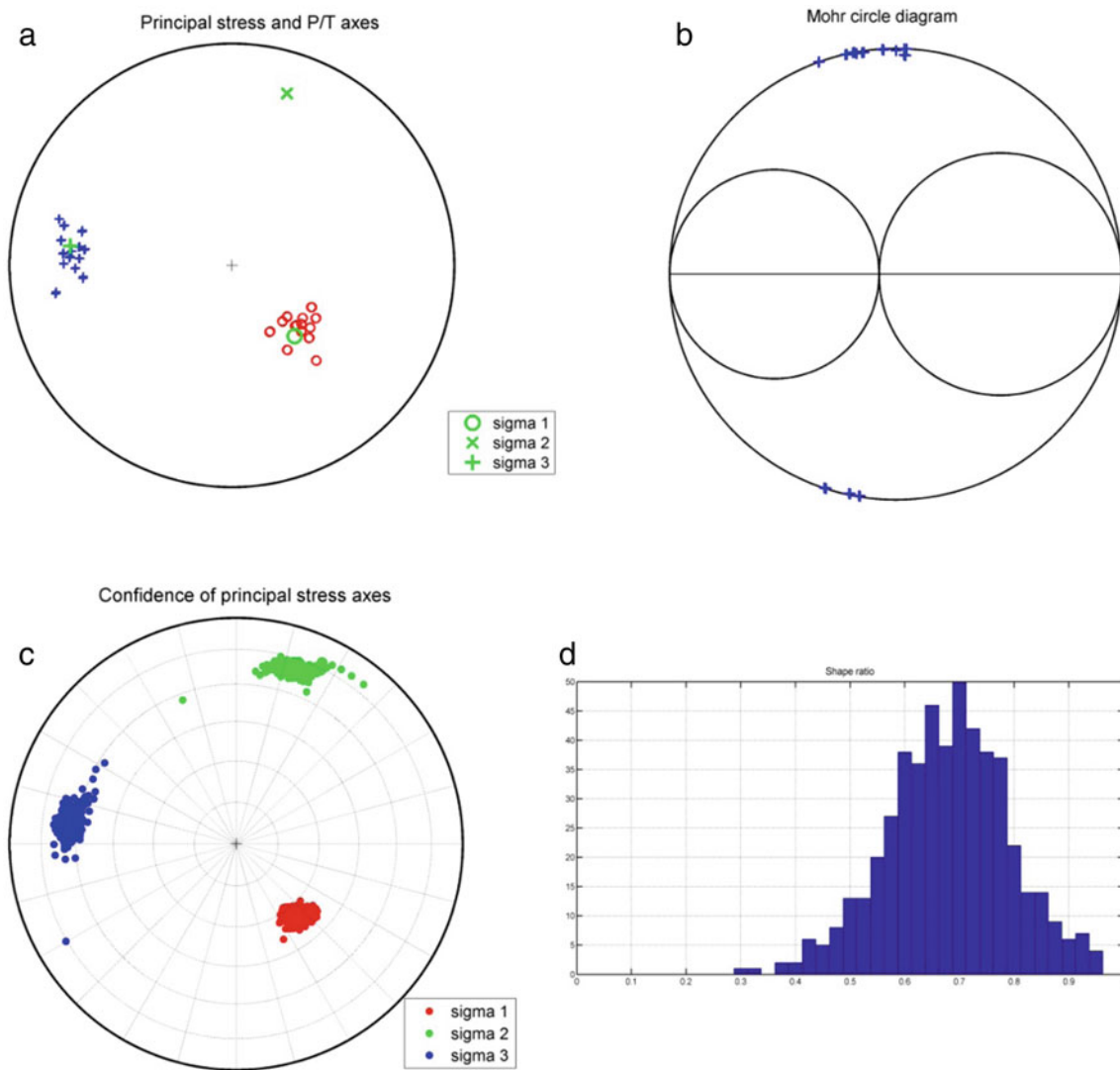northern part of Kuwait in 2019
(after Abd el-aal et al., 2021a)

Fig. 7.23 The estimated stress tensor results acquired from focal mechanism solutions in the northern region of Kuwait. The panel (**a**) illustrates the σ_1, σ_2 and σ_3 axes and P- and T axes. Panel (**b**) shows the Mohr's circles with the faults recognized by the blue crosses. Panel (**c**) shows the confidence limits of the main stress axes. Finally, the shape ratio values are mainly plotted in Panel (**d**)

Table 7.4 The azimuth and plunge values of main stress axes of the earthquakes sequence occurred at the northern area of Kuwait

Principle stress axes	Earthquake sequence	
	Azimuth	Plunge
σ_1	138.5°	54.9°
σ_2	17.7°	19.8°
σ_3	276.8°	27.6°

References

Abd el-aal, A. K., Al-Jeri, F., Al-Enezi, A., & Parol, J. A. (2020). Seismological aspects of the 15 November 2019 earthquakes sequence, Kuwait. *Arabian Journal Geoscience, 13*, 941. https://doi.org/10.1007/s12517-020-05919-1.

Abd el-aal, A. K., Parol, J. A., Al-Jeri, F., & Al-Enezi, A. (2021a). Modeling and simulating ground motion from potential seismic sources to Kuwait: Local and regional scenarios. *Geotectonics, 55*. https://doi.org/10.1134/S001685212103002X.

Abd el-aal, A. K., Al-Enezi, A., Sadalla, H., & Al-Jeri, F. (2021b). Tectonic and anthropogenic characteristics of the 15 November 2019 micro earthquakes sequence, Kuwait. *Geotectonics, 55*, 137–152. https://doi.org/10.1134/S0016852121010039.

Abd el-aal, A. K. A., Al-Enezi, A., Al-Jeri, F., & Mostafa, S. I. (2021c). Earthquake deterministic hazard and sensitivity analysis for residential Cities in Kuwait. *Journal of Volcanology and Seismology, 15*(6), 445–462. https://doi.org/10.1134/S0742046321060051.

Abd el-aal, A. K., Al-Enezi, A., Al-Jeri, F., Naser, O., & Alenezi, Mostafa, S. I. (2022). Probabilistic and deaggregation seismic hazard maps for Kuwait. *Submitted to Arabian Journal of Geosciences*.

Abdelmeinum, M. M., Abdel-Fattah, R., & Agami, D. N. (2004). "Earthquakes" Kuwait Research for Scientific Research publishing in Arabic language.

Al-enzi, A., Sadeq, A., & Abdel-Fattah, R. (2007). Assessment of the Seismic Hazard for the state of Kuwait. Internal report EC011C, submitted to KFAS 2007.

Allen, C. R. (1982). Earthquake Prediction—1982 overview. *Bulletin of the Seismological Society of America, 72*(6B), S331–S335.

Allen, M., Jackson, J. A., & Walker, R. (2004). Late Cenozoic reorganization of the Arabia-Eurasia collision and the comparison of short-term and long-term deformation rates. Tectonics 23, TC2008.

Ammon, C. J., Randall, G. E., & Zandt, G. (1990). On the non-uniqueness of receiver function inversions. *Journal of Geophysical Research, 95*, 15303–15318.

Bath, M. (1979). Introduction to Seismology (Second, Revised ed.). Basel: Birkhäuser Basel. ISBN: 9783034852838.

Berberian, M. (1995). Master 'blind' thrust faults hidden under the Zagros folds, active basement tectonics and surface morphotectonics. *Tectonophys, 241*, 193–224.

Burton, I., Kates, R. W., & White, G. F. (1978). *The Environment as Hazard*. New York: Oxford University Press.

Bolt, B. A. (1993). Earthquakes and geological discovery, *Scientific American Library*, ISBN: 978-0-7167-5040-6.

Bormann, P. (Ed.) (2012). New manual of seismological observatory practice (NMSOP-2), IASPEI, GFZ German Research Centre for Geosciences, Potsdam; nmsop.gfz-potsdam.de. https://doi.org/10.2312/GFZ.NMSOP-2.

Bou-Rabee, F. (2000). Seismotectonics and earthquake activity of Kuwait. *Journal Seismology, 4*, 133–141.

Bou-Rabee, F., & Nur, A. (2002). The 1993 M4. 7 Kuwait earthquake: Induced by the burning of the oil fields, Kuwait. *Journal Science Engineering, 29*(2), 155–163.

Bou-Rabee, F., & Abdel-Fattah, R. (2004). Seismological observation in the state of Kuwait. *Kuwait Journal Science Engineering, 31*(1), 175–192.

Cooper, M. (2007). Structural style and hydrocarbon prospectivity in fold and thrust belts: A global review. In A. C. Ries, R. W. Butler & R. H. Graham (Eds.), *deformation of the continental crust: The legacy of mike coward*. Special Publications. 272. London: Geological Society. pp. 447–472. ISBN: 978-1-86239-215-1. Retrieved 2 July 2011.

Chung, D. H., & Bernreuter, D. L. (1980). Regional Relationships Among Earthquake Magnitude Scales., NUREG/CR-1457.

Davison, C. (2014). The founders of seismology. ISBN: 9781107691490.

Dudley, W. C., & Lee, M. (1988: 1st edition) Tsunami! ISBN: 0-8248-1125-9.

Engdahl, E. R., Jackson, J. A., Myers, S. C., Bergman, E. A., & Priestley, K. (2006). Relocation and assessment of seismicity in the Iran region. *Geophysical Journal International, 167*, 761–777.

Fojtikova, L., & Vavrycuk, V. (2018). Tectonic stress regime in the 2003–2004 and 2012–2015 earthquake sequences in the Ubaye Valley, French Alps. Pure Appl Geophys. https://doi.org/10.1007/s00024-018-1792-2.

Fojtíková, L., Vavryčuk, V., Cipciar, A., & Madarás, J. (2010). Focal mechanisms of micro-earthquakes in the Dobrá Voda seismoactive area in the Malé Karpaty Mts. (Little Carpathians), Slovakia. Tectonophysics, 492(1–4), pp.213–229.

Garzica, E., Vergés, J., Sapin, F., Saura, E., Meresse, F., & Ringenbachc, J. C. (2019). Evolution of the NW Zagros Fold-and-Thrust Belt in Kurdistan Region of Iraq from balanced and restored crustal-scale sections and forward modeling. *Journal of Structural Geology, 124*(2019), 51–69.

Gok, R. M., Rodgers, A. J., & Al-Enezi, A. (2006). Seismicity and improved velocity structure in Kuwait. Internal report submitted to KISR, report no: UCRL-TR-218465.

Gu, C., Al-Jeri, F., Al-Enezi, A., Büyüköztürk, O., & Toksöz, M. N. (2017). Source mechanism study of local earthquakes in Kuwait. *Seismological Research Letters, 88*(6), 1465–1471. https://doi.org/10.1785/0220170031.

Gu, C., Prieto, G. A., Al-Enezi, A., Al-Jeri, F., Al-Qazweeni, J., Kamal, K., Kuleli, S., Mordret, A., Büyüköztürk, O., & Toksöz, M. N. (2018). Ground motion in Kuwait from regional and local earthquakes: Potential effects on tall buildings. *Pure Application Geophysics, 175*, 4183.

Gubbins, D. (1990). *Seismology and plate tectonics*. Cambridge University Press. ISBN: 978-0-521-37141-4.

Gutenberg, B., & Richter, C. F. (1942). Magnitude and energy of earthquakes. *Buletin of the Seismology Society of Amercia, 32*, 163–191.

Hall, S. S. (2011). Scientists on trial: At fault? *Nature, 477*(7364), 264–269. Bibcode:2011Natur.477.264H. https://doi.org/10.1038/477264a.

Hanks, T. C., & Kanamori, H. (1979). A moment magnitude scale. *Journal of Geophysical Research, 84*, 2348–2350.

Hatzfeld, D., Tatar, M., Priestley, K., & Ghafory-Ashtiany, M. (2003). Seismological constraints on the crustal structure beneath the Zagros Mountain belt (Iran). *Geophysical Journal International, 155*, 403–410.

Herrmann, R. B. (1973). Some aspects of bandpass filtering of surface waves. *Bulletin of the Seismology Society America, 63*, 663–671.

Hessami, K. (2002). Tectonic history and present-day deformation in the Zagros fold-thrust belt. Acta Universitatis Upsaliensis. Comprehensive Summaries of Uppsala Dissertations from the Faculty of Science and Technology 700. 13 pp. Uppsala. ISBN: 91-554-5285-5.

Hessami, K., Nilforoushan, F., & Talbot, C. J. (2006). Active deformation within the Zagros Mountains deduced from GPS measurements. *Journal of the Geological Society of London, 163*, 143–148.

Hessami, K., Jamali, F., & Tabassi, H. (2003). Major active faults in Iran. Ministry of science, research and technology. *International Institute of Earthquake Engineering and Seismol.* (IIEES), 1:250000 scale map.

Hutton, L. K., & Boore, D. (1987). The M_L scale in Southern California. *Bulletin of the Seismology Society of America, 77*, 2074–2094.

Jackson, J. A. (1980). Error in focal depth determination and the depth of seismicity in Iran and Turkey. *Geophysical Journal of the Royal Astronomical Society, 61*, 285–301.

Jackson, J. A., & McKenzie, D. (1984). Active tectonics of the Alpine-Himalayan Belt between western Turkey and Pakistan. *Geophysical Journal of the Royal Astronomical Society, 77*, 185–264.

Johnson, P. R. (1998). Tectonic map of Saudi Arabia and adjacent areas. Deputy Ministry for Mineral Resources, USGS TR-98–3, Saudi Arabia.

Kadinsky-Cade, K., & Barazangi, M. (1982). Seismotectonics of southern Iran: The Oman Line. *Tectonics, 1*, 389–412.

Kalaneh, S., & Agh-Atabai, M. (2016). Spatial variation of earthquake hazard parameters in the Zagros fold and thrust belt. *SW Iran. Nat Hazards, 2016*(82), 933–946. https://doi.org/10.1007/s11069-016-2227-y.

Kanamori, H. (1977). Energy-release in great earthquakes. *Journal of Geophysical Research, 82*, 2981–2987. https://doi.org/10.1029/Jb082i020p02981.

Kanamori, H. (2003). Earthquake prediction: An overview. International Handbook of Earthquake and Engineering Seismology. 81 Part B. *International association of seismology & physics of the earth's interior*, pp. 1205–1216.

KISR. (2019). *Annual earthquakes bulletin*. Kuwait institute of scientific Research, Kuwait.

Langston, C. A. (1979). Structure under Mount Rainer, Washington, inferred from teleseismic body waves. *Journal of Geophysical Research, 84*, 4749–4762.

Laske, G., Masters, G., & Reif, C. (2001). Crust 2.0: a new global crustal model at 2 × 2 degrees http://mahi.ucsd.edu/Gabi/rem.html.

Lay, T and Wallace, T. (1995). Modem global seismology. *Intemational Geophysics Series*, (Vol. 58). New York: AcademicPress.

Lee, W. (1990). Hypo71pc program. IASPI software library, Vol 1.

Lee, W., Kanamori, H., Jennings, P., & Kisslinger, C. (2003). International Handbook of Earthquake and Engineering Seismology, Part B. Volume 81, Part B, pp. 937–1948.

Lee, W., & Stewart, S. (1981). *Principles and applications of microearthquake networks*. Academic Press.

Levin, B., & Nosov, M. (2009). *Physics of tsunamis*. Springer, Dordrecht 2009. ISBN: 978-1-4020-8855-1.

Lienert, B. R., & Havskov, J. (1995). A computer program for locating earthquakes both locally and globally. *Seismological Research Letters, 66*, 26–36.

Michael, A. J. (1984). Determination of stress from slip data: Faults and folds. *J Geophys Res Solid Earth, 89*(B13), 11517–11526.

Ni, J., & Barazangi, M. (1986). Seismotectonics of Zagros continental collision zone and a comparison with the Himalayas. *Journal of Geophysical Research, 91*(B8), 8205–8218.

Owens, T. J., Zandt, G., & Taylor, S. R. (1984). Seismic evidence for an ancient rift beneath the Cumberland Plateau, Tennessee: A detailed analysis of broadband teleseismic P waveforms. *Journal of Geophysical Research, 89*, 7783–7795.

Pasyanos, M. E., Walter, W. R., & Hazler, S. E. (2001). A surface wave dispersion study of the Middle East and North Africa for monitoring the Comprehensive Nuclear-Test-Ban Treaty, Pure App. *Geophysics, 158*, 1445–1474.

Pasyanos, M. E., Walter, W. R., & Flanagan, M. P., Goldstein, P., & Bhattacharyya, J. (2004). Building and testingan a priori geophysical model for Western Eurasia and North Africa. *Pure and Applied Geophysics, 161*, 235–281.

Pasyanos, M. E., Tkalcic, H., Gok, R., Al-Enezi, A., & Rodgers, A. J. (2007). Seismic structure of Kuwait. *Geophysical Journal International, 2007*(170), 299–312. https://doi.org/10.1111/j.1365-246X.2007.03398.x.

Richter, C. F. (1935). An instrumental earthquake magnitude scale. *Bulletin of the Seismology Society America, 25*, 1–32.

Rodgers, A., Walter, W., Mellors, R., Al-Amri, A. M. S., & Zhangm, Y. S. (1999). Lithospheric structure of the Arabian shield and platform from complete regional waveform modeling and surface wave group velocities, *Geophysical Journal International, 138*: 871–878.

Tatar, M., Hatzfeld, D., & Ghafory-Ashtiany, M. (2004). Tectonics of the central Zagros (Iran) deduced from microearthquake seismicity. *Geophysical Journal International, 156*, 255–266. https://doi.org/10.1111/j.1365-246X.2003.02145.x.

Talebian, M., & Jackson, J. (2004). A reappraisal of earthquake focal mechanisms and active shorting in the Zagros Mountains of Iran. *Geophysical Journal International, 156*, 506–529.

Vavrycuk, V. (2011). Principal earthquakes: Theory and observations from the 2008 West Bohemia sequence. *Earth and Planetary Science Letter, 305*, 290–296. https://doi.org/10.1016/j.epsl.2011.03.002.

Vavrycuk, V. (2014). Iterative joint inversion for stress and fault orientations from focal mechanisms. *GJI, 199*(1), 69–77.

Vavrycuk, V., Bouchaala, F., & Fischer, T. (2013). High-resolution fault image from accurate locations and focal mechanisms of the 2008 sequence earthquakes in West Bohemia, Czech Republic. *Tectonophys, 590*, 189–195. https://doi.org/10.1016/j.tecto.2013.01.025.

Vergés, J., Saura, E., Casciello, E., Fernàndez, M., Villaseñor, A., Jiménez-Munt, I., et al. (2011). Crustal-scale cross-sections across the NW Zagros belt: Implications for the Arabian margin reconstruction. *Geological Magazine, 148*(5–6), 739–761.

Vernant, Ph., Nilforoushan, F., Hatzfeld, D., Abassi, M. R., Vigny, C., Masson, F., Nankali, H., Martinod, J., Ashtiani, A., Bayer, R., Tavakoli, F., & Chery, J. (2004). Present-day crustal deformation and plate kinematics in Middle East constrained by GPS measurements in Iran and northern Oman. *Geophysics Journal Interncational, 157*, 381–398.